LABORATORIUM VOOR SCHEEPSCONSTRUCTIES

TECHNISCHE HOGESCHOOL – DELFT

RAPPORT Nr. SSL 161

BETREFFENDE:

Investigations regarding the possibility of the use of test-specimens with reduced dimensions in the Niblink method of testing.

By dr.eng. S. Kubera.

SHIP STRUCTURES LABORATORY,
Delft University of Technology,
Mekelweg 2, Delft,
The Netherlands.

Report no. **SSL 161**

INVESTIGATIONS REGARDING THE POSSIBILITY OF THE USE OF TEST-SPECIMENS WITH REDUCED DIMENSIONS IN THE NIBLINK METHOD OF TESTING.

by

S. Kubera.

July 1971.

CONTENTS:

INVESTIGATIONS REGARDING THE POSSIBILITY OF THE USE OF TEST-SPECIMENS WITH REDUCED DIMENSIONS IN THE NIBLINK METHOD OF TESTING.

By S. Kubera. *

1. Introduction.

The NIBLINK method of testing /1/ is intended for testing low strength ferritic steels. The method is useful for estimation of critical regions of weldments from the viewpoint of brittle fracture danger.

In the above method of testing, the dimensions of a test-piece were determined rather intuitively, including two important parameters, viz. the plate thickness and full cross-section of the weldment. The results of numerous of the tests carried out in different laboratories /2-7/, indicated the specific features of the method as well as the limits of application. Some reservation still exists concerning the procedure of the testing because of the not very clear physical meaning of the crack opening displacement (COD) value measured by the tests, obtained on the test-piece as the result of repeated impact loading /8/.

The present paper deals with the research carried out in the Delft University of Technology, Ship Structures Laboratory, with the purpose to prove the possibility of reduction of the specimen-dimensions in the NIBLINK test-procedure. Simultaneously the purpose of the investigations was the collection of some special information enabling the better understanding and interpreting of the values measured by the tests. For these reasons the experiments were carried out applying more complicated methods of measurements than the usual NIBLINK testing-method /10/.

2. Assumptions for the tests.

2.1. Material and dimensions of the test-specimen.

All specimens were made from the same plate of a low carbon steel of a thickness t = 30 mm.
The yield-point for the plate material was 25,4 kg/mm^2 and the tensile strength 40,4 kg/mm^2.

For the comparison tests, regarding the possibility of reduction of the test-specimen dimensions (fig. 1), two series of the test-specimens were used.

Series 1: with reduced height only, consisting of three groups of specimens:

- NIBLINK specimen (N-B/1) h = 65 mm, s = 325 mm
- intermediate specimen (M/1) h = 40 mm, s = 325 mm
- small specimen (S/1) h = 20 mm, s = 325 mm.

Series 2: with reduced height and length:

- N-B/2 h = 65 mm, s = 325 mm
- M/2 h = 40 mm, s = 228 mm
- S/2 h = 20 mm, s = 152 mm.

* Dr.Eng., Naval Architect.
Gdansk Technical University, Ship Research Institute, Gdansk, Poland.

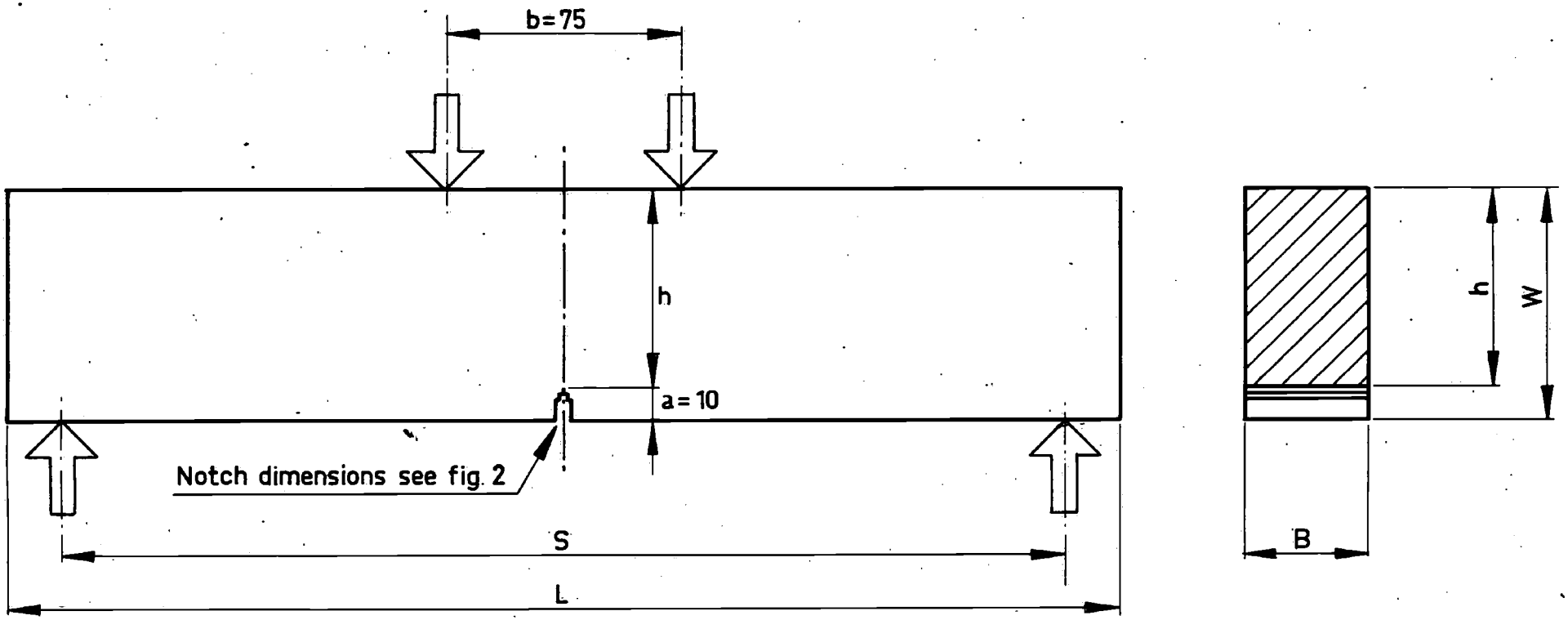

FOR NIBLINK TEST SPECIMEN: h=65 ; W=75 ; S=325 ; L=360 ; B= thickness of the plate.

FIG:1 The dimensions of the test piece.

150

Fig 1/R2

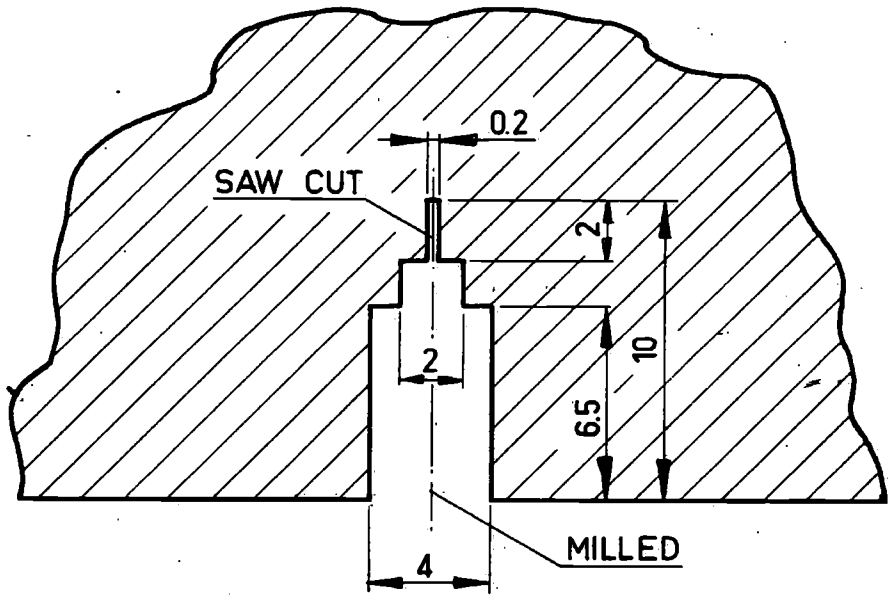

FIG: 2 The dimensions of the notch

70

FIG 2 /R2

Fig. 1

All the specimens had the same notch dimensions as the NIBLINK test piece (fig. 2)..

The breadth (B) of all of the specimens was constant and equal to the thickness of the plate (30 mm).

Fig. 2

The dimensions of the S/2 specimen correspond nearly to the dimensions of a standard test-piece for COD-testing recommended by the CODA-panel /9/. According to this proposal, the specimen should be of square cross-section (B = W); the loading span (S) should be 4× the specimen-width (W) and the notch-depth: $a = \frac{W}{3}$.

2.2. Test conditions for series 1 and 2.

In the NIBLINK-test, the drop-hammer mass is related to the plate thickness and corresponds to a weight in kg equal to the plate thickness in mm. Hence for N-B specimen used in the investigations, the drop-hammer weight was fixed as P = 30 kg. For the specimens with reduced dimensions, the drop-weight was decreased relative to the cross-section reduction.

It means that for all the specimens the following criterion was fulfilled:

$\frac{\text{energy of blow}}{\text{notch cross-section}}$ equal for the same height of blow.

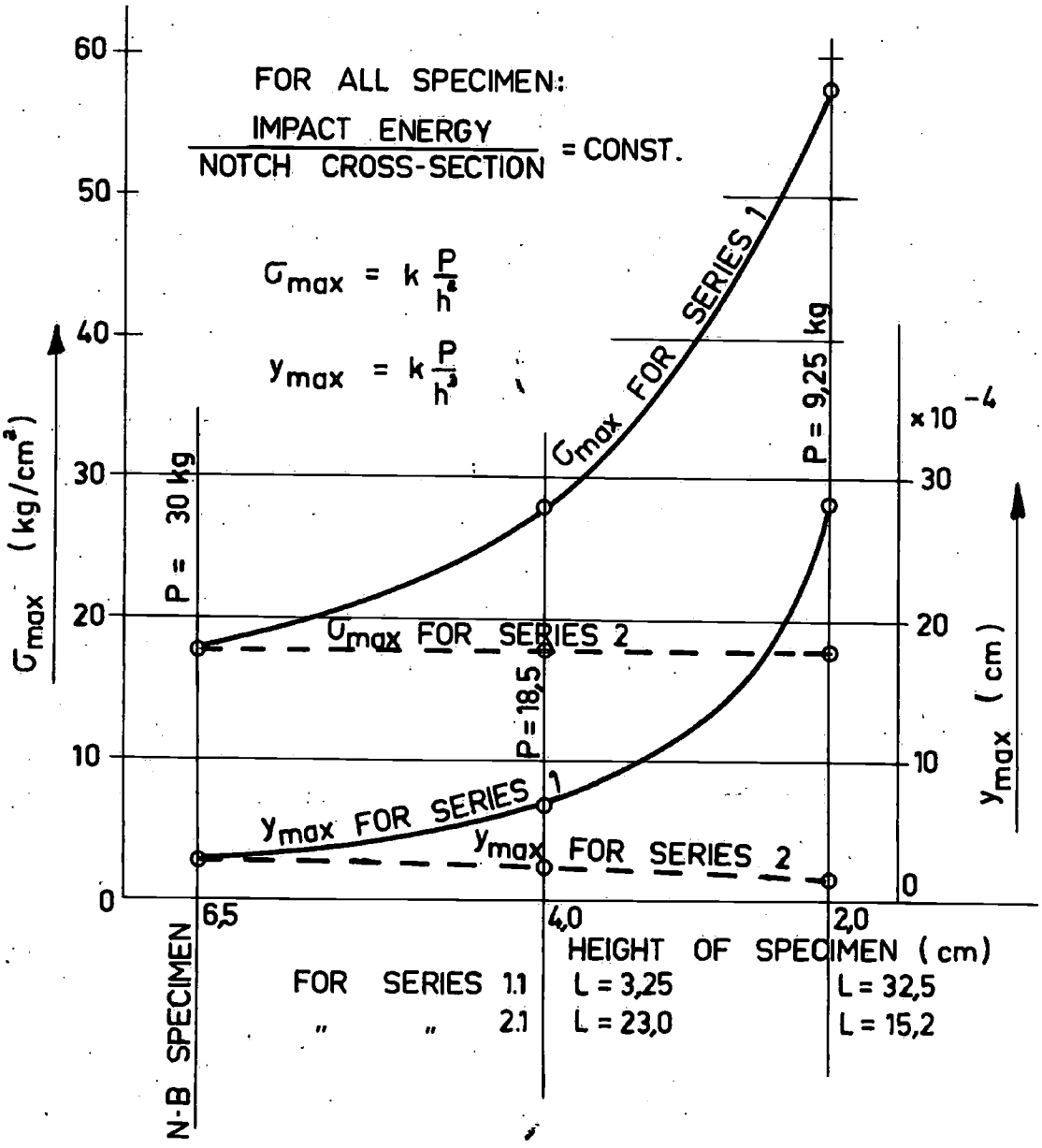

FIG:3 Comparison of the σ_{max} and y_{max} for the specimen: series 1 and 2.

FIG 3/R2

For specimens of series 2, additionally two other criteria were fulfilled: equal σ_{max} and y_{max}, for the same height of blow. (σ_{max} is the maximum bending stress in notch cross-section, y_{max} is the deflection of the specimen, calculated for static conditions). (Fig. 3).

Fig. 3

According to the NIBLINK test procedure, the height of the first blow for all specimens was the same (H = 20 cm) and for the following blows increased in steps of ΔH = 5 cm or ΔH = 10 cm.

All the specimens in series 1 were tested at room temperature (T = +20°C). One part of the specimens in series 2 was tested at low temperatures (T = 0°, -10°, -20°, -30°, -40°C).

Specifications of the specimens of series 1 and series 2 are given in table I (appendix 1).

2.3. Welded specimens series with reduced dimensions.

The fundamental advantage of a specimen of the NIBLINK-type is that such a specimen with its dimensions is sufficiently sensitive to give real information regarding the resistance of the tested material to fracture initiation. The NIBLINK-type specimen is especially useful for tests of all regions of weldment which can be critical, (these are HAZ, weld-metal or parent plate material).
To check if this feature is not changed by reduction of the specimen-dimensions, a second stage of investigations was realized with use of welded specimens (type W), with the dimensions like for the specimens of type S.

All the test-joints were welded manually. The weldments were prepared by use of electrode-type CONARC 51 of higher strength (50-60 kg/mm^2), or electrode-type RESISTENS of lower strength (45-50 kg/mm^2). For each elec-

STRAIN GAUGES ON SPECIMENS FOR CALIBRATION

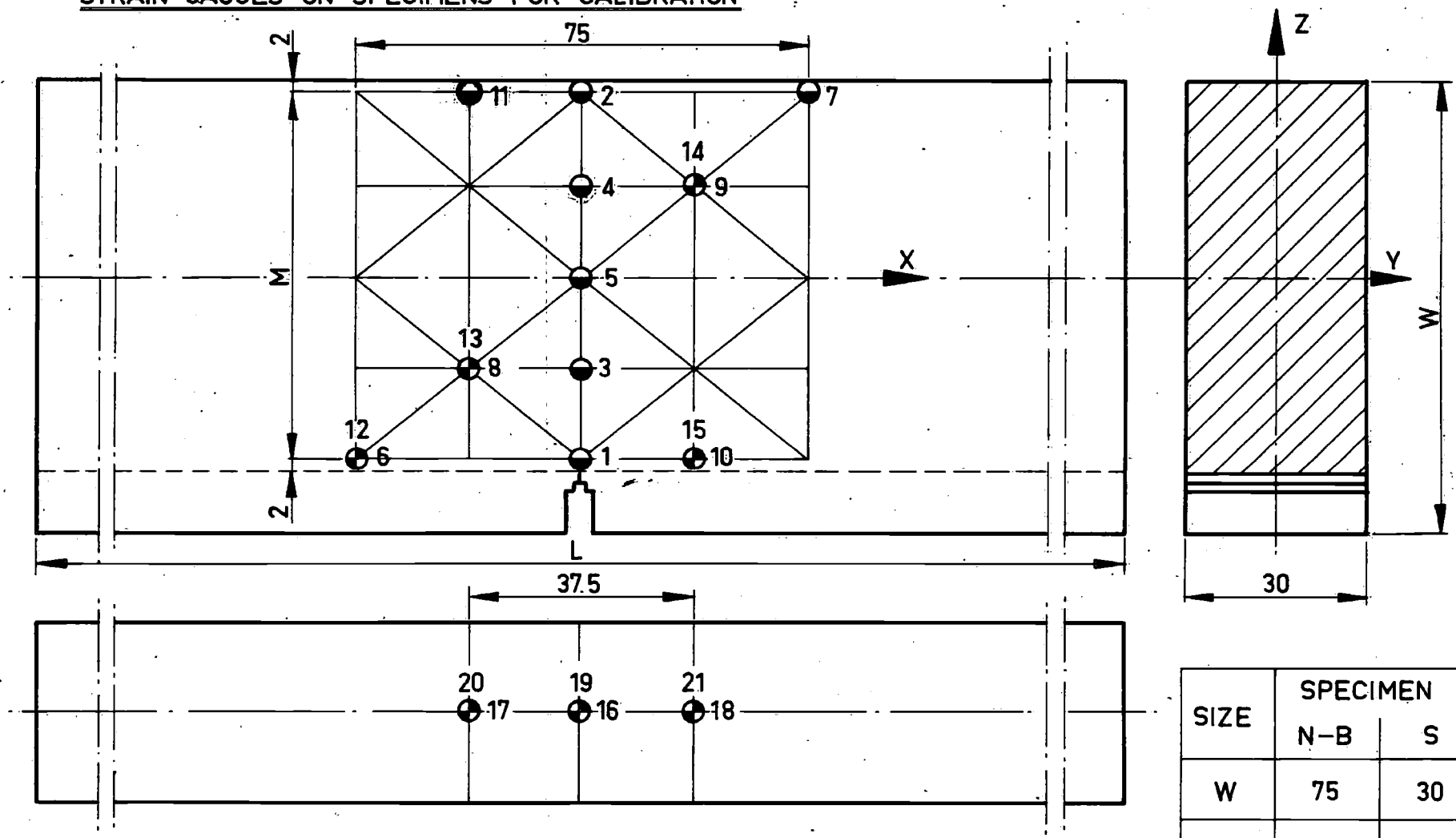

SIZE	SPECIMEN	
	N–B	S
W	75	30
L	360	180
M	61	16

NOTATION :

- Strain gauge type PL.3 in direction X
- Strain gauge type PC.5 in direction X and Y or Z

FIG. 4 Location of the strain gauges on the specimen for calibration test.

FIG 4/R 2

trode one welded plate was made at room temperature (T = +20°C), and one at lower temperature (T = 0°C). The specimens were machined with a notch cross-section in the weld-axis or in the HAZ (10 mm from the weld-axis).

All the welded specimens were tested at the following temperatures: +20°, 0°, -20° and -40°C.

Specifications of the welded specimens are given in table II (appendix 1).

3. Test procedure.

3.1. Instrumentation of the drop-weight test.

In a conventional NIBLINK test procedure one variable is determined, namely the Crack Opening Displacement (COD), being the residual value after a blow, measured in the region of the notch. The COD-value is measured by means of a special COD-dial gauge.

For the investigations being the subject of this report, special instrumentation was applied for measurement of the impact force transmitted to the test-specimen by a blow and for measurement of the dynamical COD-value which corresponds to this force.*)

By tests at low temperatures, the temperature of the specimen was checked by means of a thermocouple connected directly to the specimen.

3.2. Calibration tests.

In the first stage of the investigations it was of special interest to recognize the dynamical behaviour of a test-specimen under an impact loading and also to confirm that there is an essential similarity between phenomena occurring at tests on a normal specimen and on a specimen with reduced dimensions.

For this purpose two specimens (N-B and S) were used with 21 strain gauges fixed at corresponding points on both of the specimens (fig. 4).

Fig. 4

*). See report no. 160.

In consequence of the above calibration, all the specimens of series 1 and 2 were tested applying one strain gauge in the region of the notch.

For determining the relation between the force, COD and deflection for the specimen, two specimens (N-B and S) were tested in static conditions.

4. Results of the calibration tests.

From the calibration tests on the N-B and S specimens, useful information was obtained regarding the magnitude of the strains in the particular points of the specimens, caused by the successive blows.

The diagrams of fig. 5 and fig. 6 show the distribution of the strains in the notch cross-sections for both kinds of the test-pieces. The diagrams, basically, are similar but there is a distinct higher intensity of the strain-increase for the smaller specimen (fig. 7).

This effect may be explained as the greater influence of the notch depth in consequence of the reduction of the specimen-height. Confirming the above conclusion may be the phenomenon of a distinct shift of the actual neutral axis for the smaller specimen shown on diagram fig. 7.

The diagrams fig. 8 and fig. 9 show the changes in the magnitude of the maximum strain (ε_{max}) in the particular points of the notch cross-section, respectively for the N-B and S-specimen. This maximum value of strain is the sum of the elastic and the residual value:

$$\varepsilon_{max} = \varepsilon_E + \varepsilon_R.$$

Both the values ε_E and ε_R were recorded during the tests. As is visible on the diagrams fig. 10, 11 and 12, there is a fundamental difference in the development of these two values. It is worthy to notice the high degree of similarity in the form of the curves of ε_E and ε_R for both the specimens.

Besides the strain measurements the magnitude of the impact force (F_{max}) and the residual COD (the last with aid of the special COD-dial gauge) were also measured. On fig. 13 there is a dimensionless comparison of the residual strains (ε_R) indicated by the strain gauge at the tip of the notch (No. 1), and the COD_R-value, for the consecutive blows. From this it may be concluded that only in the very early stage of the process, there is a linear correlation between these two values.

The strain gauges located at some distance from the notch cross-section (in the regions where only elastic strains occur), indicated the analogy of the strain-magnitude in these points and of the magnitude of the impact force for corresponding blows (fig. 14).

The impact force curve in the final stage of the process shows an abrupt deflection for both the specimens. This is caused by the reduction of the stiffness of the specimen at the beginning of the fracture. It can be expected that by the first blows, when the elastic deflection of the specimen is predominant, the impact force will be linearly depending on the square root of the energy of the blow (En). As is visible on the diagram fig. 15 (giving the impact force as a function of En), the values of the impact force indeed approach to the straight line for the first stage of the process.

On the diagram fig. 16 the impact force (F_{max}) related to the height of the specimen for both specimens was expressed as function of COD_R.

From this diagram may be noticed the relative higher loading of the specimen S, what is in good agreement with the picture of the phenomena resulting from the strain distribution in the notch cross-section for both the specimens (fig. 5 and 6).

5. Results of the tests carried out on the specimens series 1 and 2.

In the series 1 and 2 altogether 42 test-pieces were tested. (Fig. 17 and 18).

Records were obtained of the dynamical and residual COD-value (COD_{max} and COD_R respectively) as function of the time, the impact force (F), and the strains in the tip of the notch.

The diagrams (fig. 20 till 36 - appendix) show the results of the above values measured for each of the test-pieces group with different dimensions.

It is visible that for the test-pieces series 1 (NB/1; M/1; S/1 - fig. 21, 22, 23) the reduction of the specimen height involved a distinct increase of the COD-value and the strains in the notch tip (fig. 29 and 30). As result of the higher degree of the deformations in the region of the notch, the specimens type M/1 and S/1 fractured after a smaller number of blows. Simultaneously for the specimen with reduced height, a reduction of the impact force was noticeable (fig. 31, 34).

In consequence of the length-reduction, the test-pieces in series 2 (M/2 and S/1, fig. 24, 25), indicated a less severe increase of the COD- and strain-values, and also a corresponding increase of the impact force (fig. 35, 36). The results for the specimens series 2 better approach to values for the N-B test pieces, but the analogy was still not satisfactory (fig. 19) because of the too high COD rate increase.

For all the groups, the specimens tested under the condition of height of the blow-increase $\Delta H = 5$ cm indicated higher values of COD than the specimens tested for $\Delta H = 10$ cm, for equal height of blow.

By the tests at low temperatures, the results for the N-B test-pieces were rather easier for interpretation because of more blows to the fracture, as compared to the S/2 specimens (fig. 23, 25, 28, 31). Generally speaking it seems that the slope of and the deviation from the straight part of the COD-curve are more valuable to make comparisons than only the COD-value for the last blow. The scatter in the magnitude of the COD for the last blow is visible also on the diagrams regarding the dynamical COD measurements (fig. 27), and in particular for the tests at low temperatures (fig. 26, 28).

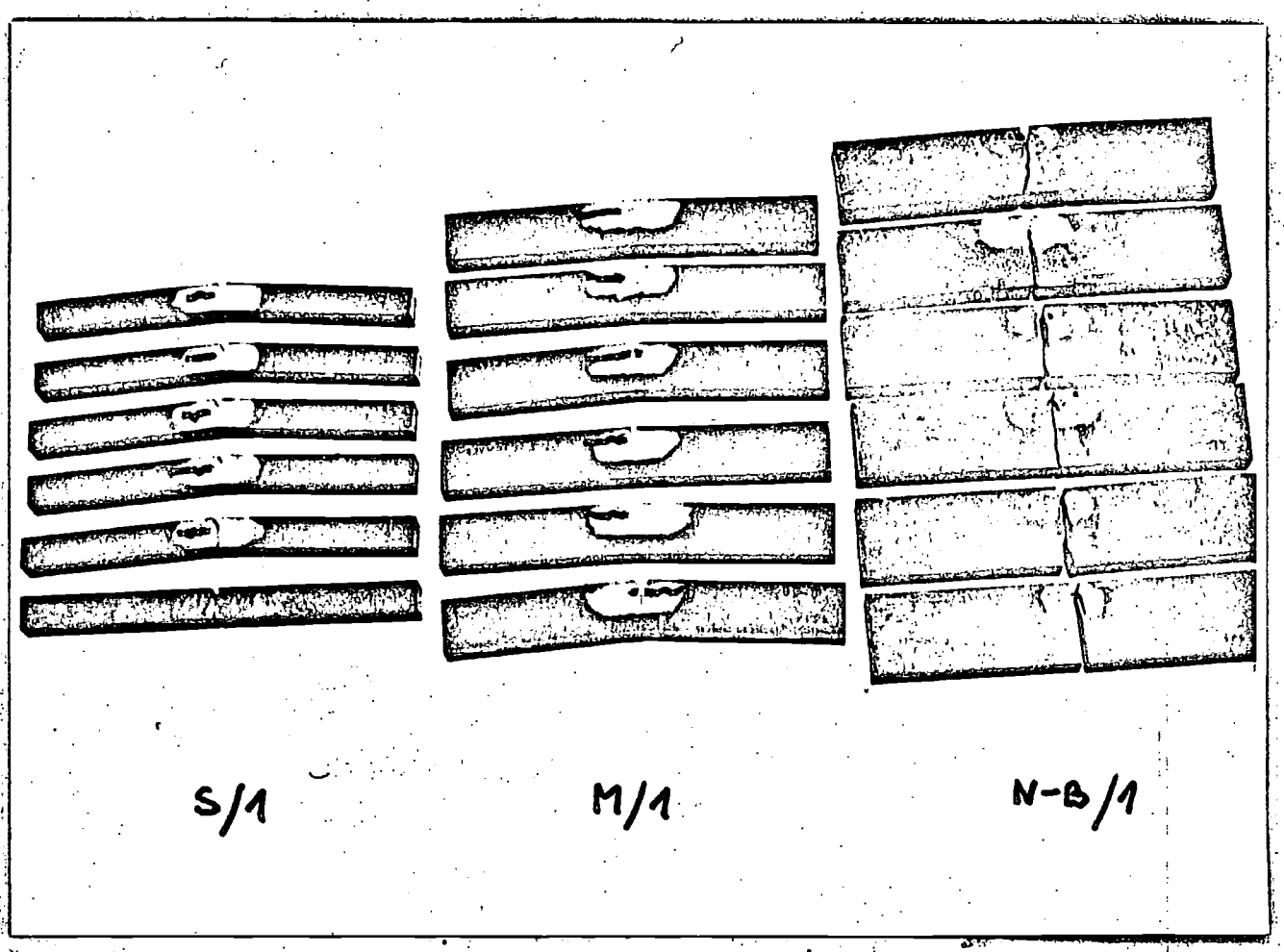

FIG: 17 Specimens of the series 1 after tests.

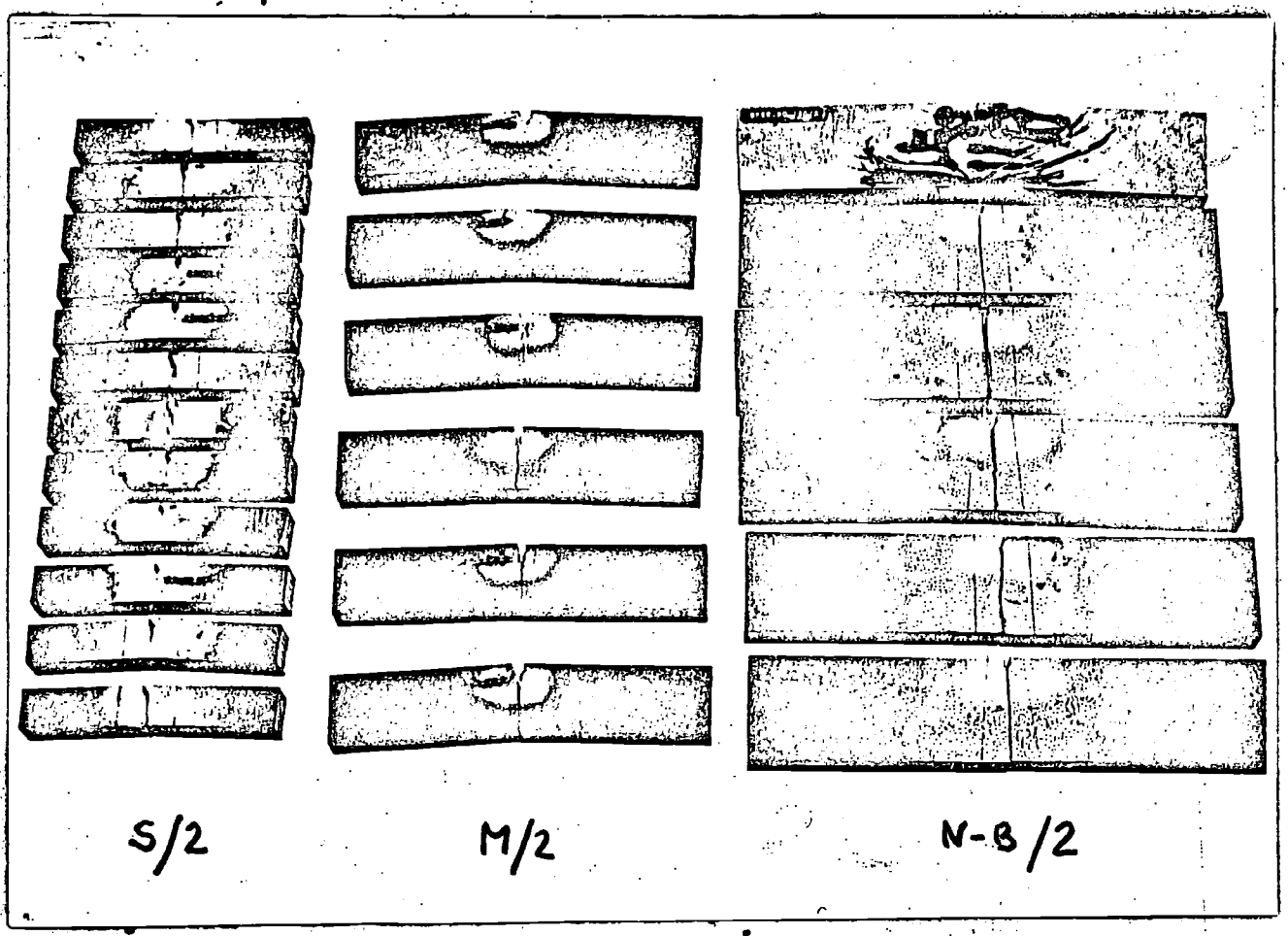

FIG: 18 Specimens of the series 2 after tests.

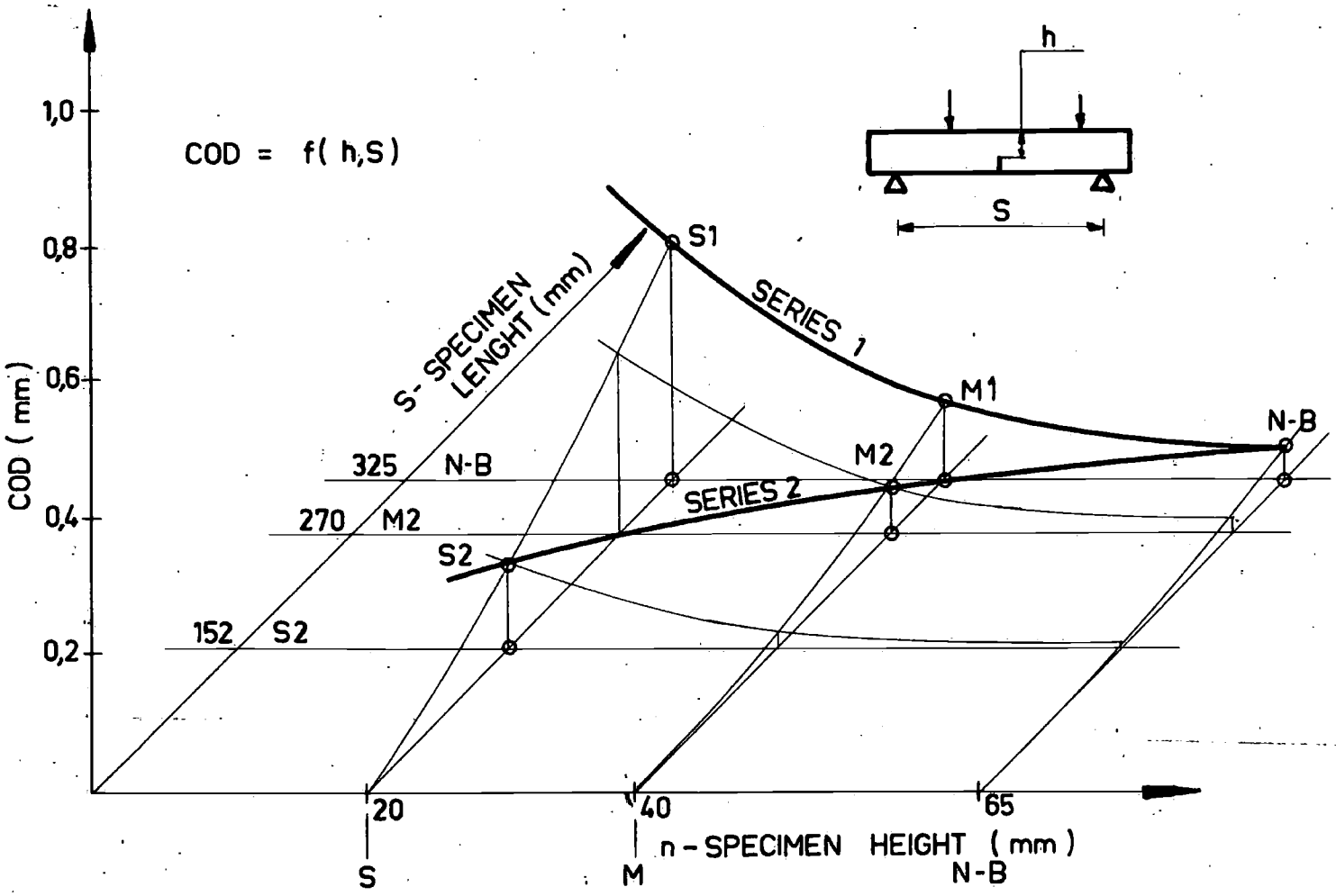
COD = f(h,S)
h
S
1,0
0,8
0,6
0,4
0,2
COD (mm)
S - SPECIMEN LENGHT (mm)
S1
SERIES 1
M1
N-B
325 N-B
M2
SERIES 2
270 M2
S2
152 S2
20
40
65
n - SPECIMEN HEIGHT (mm)
S
M
N-B

160

FIG 19/R 2

6. Results of the tests carried out on the welded specimens.

Altogether 32 of the welded test-specimens with the dimensions like for the specimens group S/2 (fig. 37) were tested.

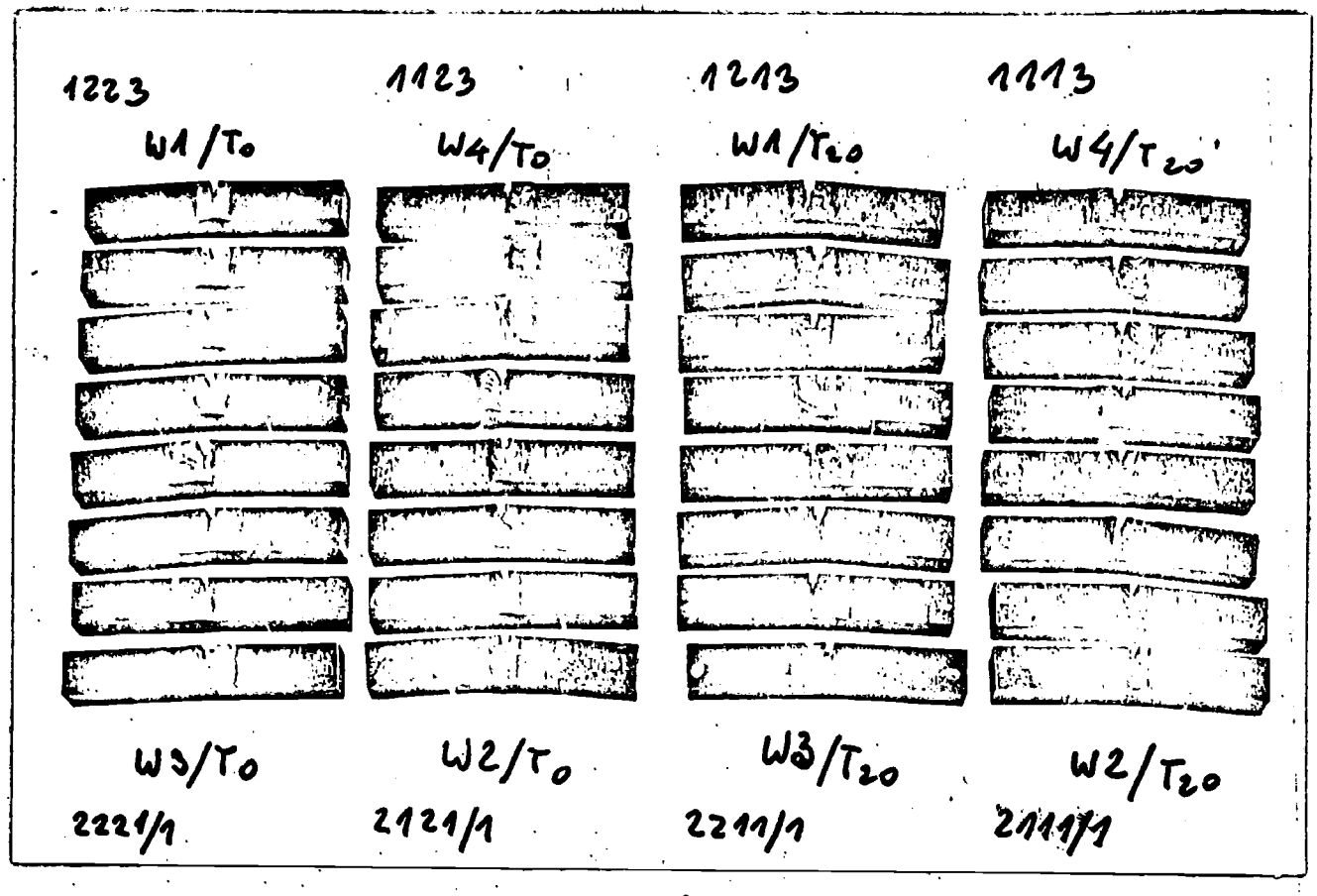

FIG:37 The specimen for investiqetion of the COD-value for the weld-metal and for the HAZ.

The comparison of the results for the welded specimens (fig. 38 till 41) is interesting because it indicates clearly that the method of testing is reliable enough to assess properties of the weldments. The results of the tests allow to distinguish not only rather rough differences between weld-metal and HAZ, but also more refined differences as the quality of the weld-metal (better results for the CONARC 51 electrode), property of HAZ (better for RESISTENS electrode) and the influence of the welding conditions (worse results for the specimens welded at low temperature: T = 0°C in comparison to the specimens welded at T = +20°C).

7. Conclusions from the tests.

The tests were carried out on the test-pieces of one kind of the steel and of once the thickness of the plate. This gives some limitations for generalization of the results.

The specimens with reduced dimensions were rather less favourable in comparison with the NIBLINK test specimen, because of too high rate of increase of the COD-value for the consecutive blows. This disadvantage, it seems, is easy to remove by changing the depth and sharpness of the notch. More satisfying results can be obtained also by the reduction of the steps of

the increase of the impact loading by test.

In any case the results from the welded specimens allow of the conclusion that the specimen with reduced dimensions (in such a way that height of the specimen = thickness of the plate; and span length of the specimen = 4× height) may find application and may replace the specimen of NIBLINK type, provided that some additional tests will be carried out to define more accurately the requirements for the specimens and to establish the optimum conditions for the tests procedure.

References.

/1/ Van den Blink, W.P. and J.J.W. Nibbering:
"Proposal for the testing of Weld Metal from the Viewpoint of Brittle Fracture Initiation".
Metal Construction, 1969.

/2/ Guerrera, V., U. Girardi and L. Savarese:
"Different Types of Niblink and Longitudinal Drop Weight Tests on Submerged Arc Weld for Determination of Brittle Fracture Initiation Temperature".
I.I.W. Doc. 2912-124-69.

/3/ Müncner, L. and J. Vrbensky:
"Brittle Fracture Initiation of Weld Metal Using Niblink Testing Method".
I.I.W. Doc. II-C-2912-70.

/4/ Ingham, T. and B. Watkins:
"Testing of Weldments Using Standard COD and Niblink Test Pieces".
I.I.W. Doc. 2912-13c-69.

/5/ Frederick, G. and R.V. Salkin:
"Réflexions sur Deux Essais COD Dynamiques".
Centre National de Recherches Métallurgiques RA 774/70.

/6/ Düren, C.:
"Some Aspects Regarding the Niblink-Test Procedure".
I.I.W. Doc. 2912-113-69.

/7/ Düren, C.:
"Behaviour of Brittle Fracture of Welded Joints on Steel St. 52-3 in the Niblink Test, Impact Test and Pellini Test".
I.I.W. Doc. 2912-146-70.

/8/ Baker, R.G., M.G. Dawes, R.E. Dolby, G.R. Egan, J.D. Harrison and G.G. Saunders:
"An Assessment of Brittle Fracture Testing Techniques".
I.I.W. Doc. 2912-137-69.

/9/ "The Use of Critical Crack Opening Displacement Techniques for the Selection of Fracture Resistant Materials".
First report of the CODA panel, 1969.

/10/ Kubera, S.:
"Measurements of Dynamic Crack Opening Displacements of Notched Steel Test Specimens under Impact Loading, According to the "Niblink" Test Procedure".
S.S.L. report no. 160, July 1971.

/11/ Burdekin, F.M., R.E. Dolby and G.R. Egan:
"Fracture Initiation in Welded Joints".
Conference on Fracture, Brighton 1970.

/12/ Kanazawa, T., S. Machida, S. Momota and Y. Hagiwara:
"A Study of the C.O.D. Concept for Brittle Fracture Initiation".
Conference on Fracture, Brighton 1970.

APPENDIX.

TABLE I. The Specimens Series 1 and 2.

	No.	specimen no.	h (cm)	S (cm)	P (kg)	Δ H (cm)	T (^{o}C)	blow to fracture	H_{max} (cm)	E_{max} (kg/cm)	Σ En (kg/cm)
	1	120/1	6,5	32,5	30	5	- 30	5	40	1.200	4.500
Cal.	2	120/2	6,5	32,5	30	10	+ 20	12	130	3.900	27.000
	3	120/3	6,5	32,5	30	5	0	13	80	2.400	19.500
	4	120/4	6,5	32,5	30	5	- 10	9	60	1.800	10.800
	5	120/5	6,5	32,5	30	5	- 20	11	70	2.100	14.850
	6	120/6	6,5	32,5	30	5	- 40	4	35	1.050	3.300
	7	110/1	6,5	32,5	30	10	+ 20	9	100	3.000	16.200
	8	110/2	6,5	32,5	30	5	+ 20	24	135	4.050	55.900
	9	110/3	6,5	32,5	30	5	+ 20	18	105	3.150	33.750
	10	110/4	6,5	32,5	30	10	+ 20	10	110	3.300	19.500
	11	110/5	6,5	32,5	30	10	+ 20	11	120	3.600	23.100
	12	110/6	6,5	32,5	30	5	+ 20	17	100	3.000	30.600
	13	111/1	4,0	32,5	18,5	10	+ 20	7	80	1.480	6.475
	14	111/2	4,0	32,5	18,5	10	+ 20	7	80	1.480	6.475
	15	111/3	4,0	32,5	18,5	10	+ 20	7	80	1.480	6.475
	16	111/4	4,0	32,5	18,5	5	+ 20	12	75	1.385	10.550
	17	111/5	4,0	32,5	18,5	5	+ 20	9	60	1.110	6.660
	18	111/6	4,0	32,5	18,5	5	+ 20	11	70	1.295	9.161
	19	121/1	4,0	22,8	18,5	10	+ 20	8	90	1.665	8.140
	20	121/2	4,0	22,8	18,5	10	+ 20	9	100	1.850	9.990
	21	121/3	4,0	22,8	18,5	10	+ 20	9	100	1.850	9.990
	22	121/4	4,0	22,8	18,5	5	+ 20	13	80	1.480	12.029
	23	121/5	4	22,8	18,5	5	+ 20	12	75	1.387	10.549
	24	121/6	4	22,8	18,5	5	+ 20	13	80	1.480	12.029
	25	112/1	2	32,5	9,25	10	+ 20	7	80	740	3.240
	26	112/2	2	32,5	9,25	10	+ 20	7	80	740	3.240
	27	112/3	2	32,5	9,25	10	+ 20	6	70	650	2.500
	28	112/4	2	32,5	9,25	5	+ 20	10	65	600	3.930
	29	112/5	2	32,5	9,25	5	+ 20	11	70	650	4.580
	30	112/6	2	32,5	9,25	5	+ 20	9	60	555	3.330
	31	122/1	2	15,2	9,25						
	32	122/2	2	15,2	9,25	5	+ 20	10	65	600	3.930
Cal.	33	122/3	2	15,2	9,25	10	+ 20	8	90	832	4.070

TABLE I. (Continuation).

The Specimens Series 1 and 2.

No.	specimen no.	h (cm)	S (cm)	P (kg)	Δ H (cm)	T (^{o}C)	blow to fracture	H_{max} (cm)	E_{max} (kg/cm)	Σ En (kg/cm)
34	122/4	2	15,2	9,25	10	+ 20	5	60	555	1.850
35	122/5	2	15,2	9,25	10	+ 20	6	70	650	2.500
36	122/6	2	15,2	9,25	10	+ 20	6	70	650	2.500
37	122/7	2	15,2	9,25	5	- 40	2	25	230	415
38	122/8	2	15,2	9,25	5	0	8	55	510	2.770
39	122/9	2	15,2	9,25	5	- 30	2	25	230	415
40	122/10	2	15,2	9,25	5	- 20	4	35	325	1.020
41	122/11	2	15,2	9,25	5	- 10	6	45	416	1.800
42	122/12	2	15,2	9,25	5	0	7	50	462	2.265

TABLE II. The Specimen Series W.

No.	specimen no.	notch	electr.	T_{weld} °C	T_{test} °C	Δ H cm	blow to fracture	H_{max} cm
1	2111/1	W	60	20	20	5	36	200
2	2111/2	W	60	20	0	5	26	145
3	2112	W	60	20	- 20	5	16	95
4	2113	W	60	20	- 40	5	11	70
5	1111/1	HAZ	60	20	20	5	7	50
6	1111/2	HAZ	60	20	0	5	4	35
7	1112	HAZ	60	20	- 20	5	4	35
8	1113	HAZ	60	20	- 40	5	1	20
9	2121/1	W	60	0	20	5	36	200
10	2121/2	W	60	0	0	5	28	155
11	2122	W	60	0	- 20	5	23	130
12	2123	W	60	0	- 40	5	7	50
13	1121/1	HAZ	60	0	20	5	5	40
14	1121/2	HAZ	60	0	0	5	2	25
15	1122	HAZ	60	0	- 20	5	2	25
16	1123	HAZ	60	0	- 40	5	3	30
17	1211/1	W	40	20	20	5	17	100
18	1211/2	W	40	20	0	5	14	85
19	1212	W	40	20	- 20	5	9	60
20	1213	W	40	20	- 40	5	4	35
21	2211/1	HAZ	40	20	20	5	10	65
22	2211/2	HAZ	40	20	0	5	6	45
23	2212	HAZ	40	20	- 20	5	6	45
24	2213	HAZ	40	20	- 40	5	1	20
25	1221/1	W	40	0	20	5	18	105
26	1221/2	W	40	0	0	5	14	80
27	1222	W	40	0	- 20	5	6	45
28	1223	W	40	0	- 40	5	1	20
29	2221/1	HAZ	40	0	20	5	8	55
30	2221/2	HAZ	40	0	0	5	4	35
31	2222	HAZ	40	0	- 20	5	3	30
32	2223	HAZ	40	0	- 40	5	1	20

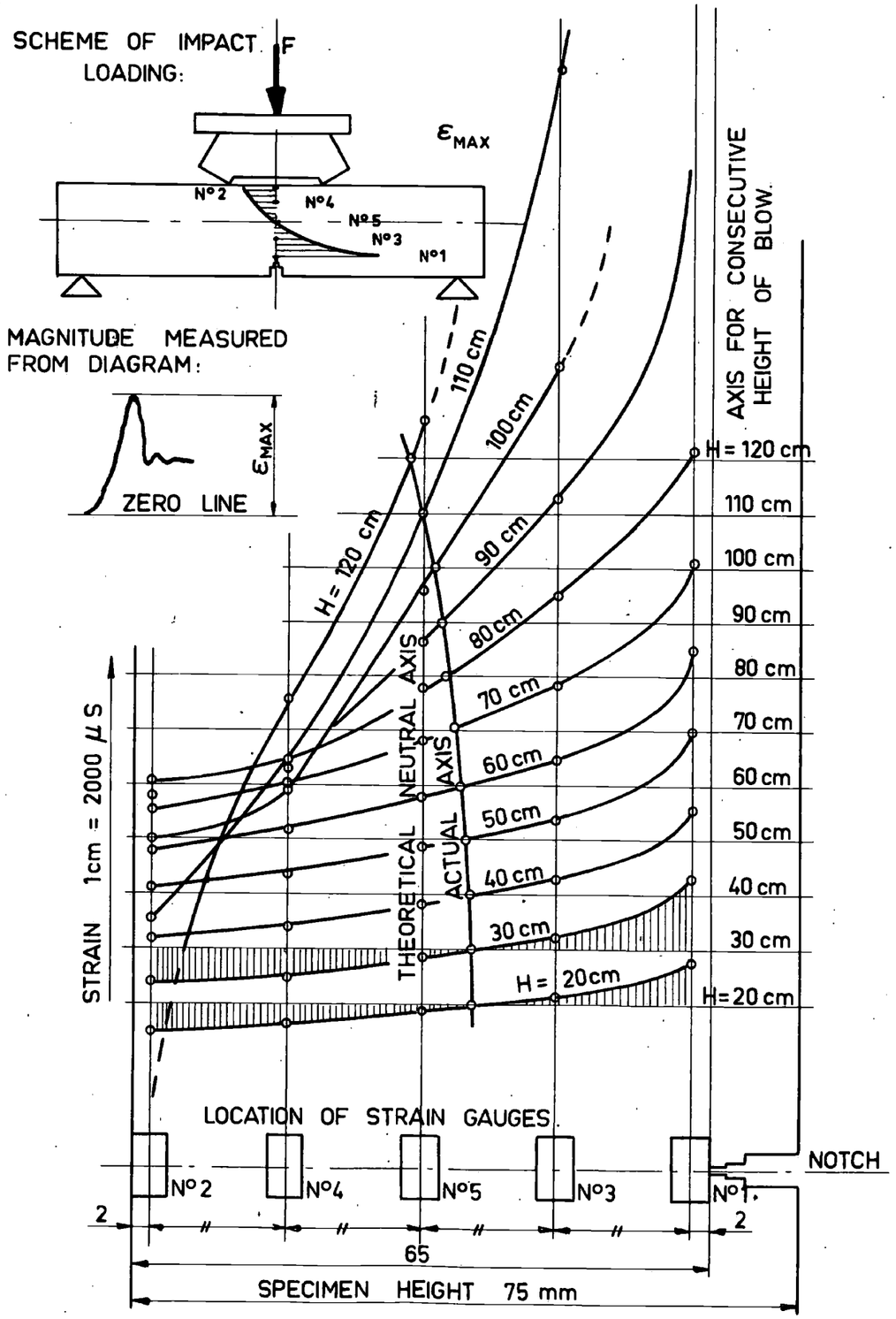

FIG. 5. Distribution of the maximum bending strain (E max) in the notch cross-section of the N-B specimen for consecutive heights of blow.

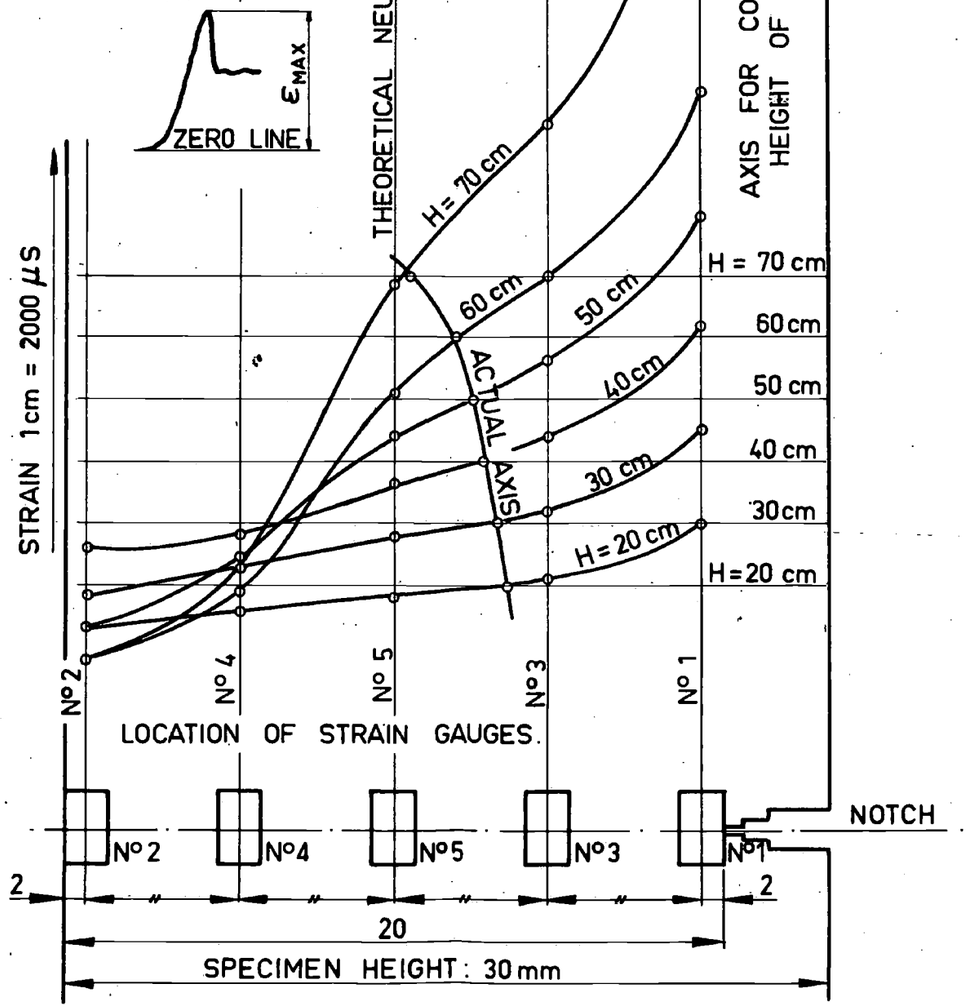

FIG. 6. Distribution of the maximum bending strain (E max) in the notch cross-section of the specimen S for consecutive heights of blow.

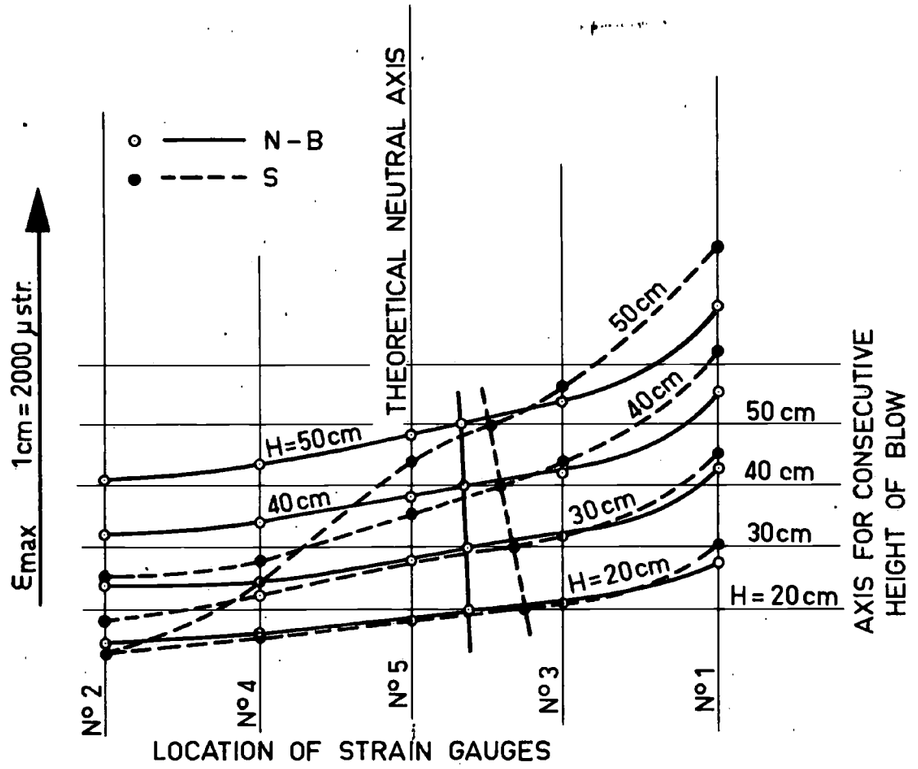

FIG. 7. Comparison of the maximum bending strains in the notch cross-section of the N-B and S specimens, for heights of blow H = 20, 30, 40 and 50 cm.

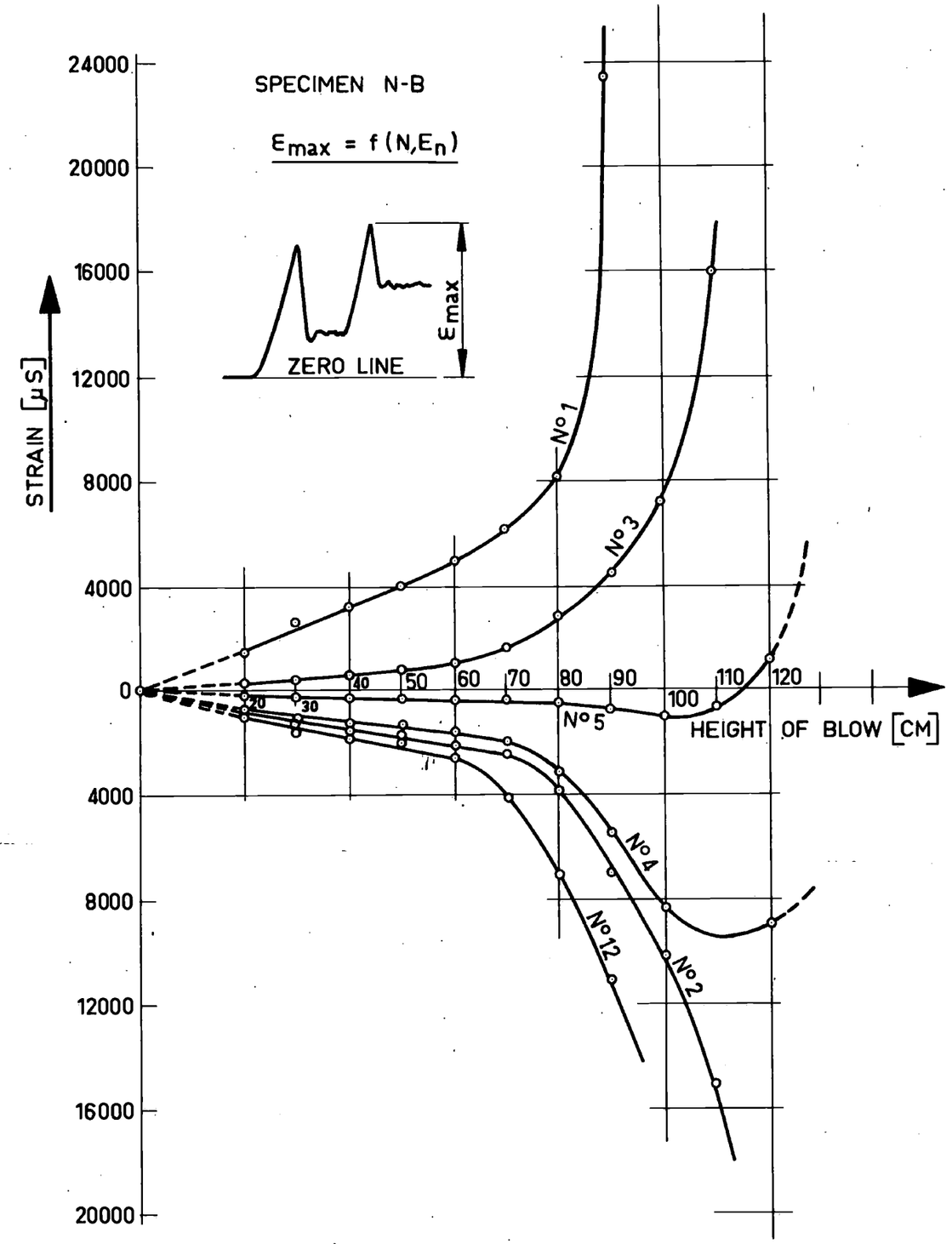

FIG. 8. Maximum strains in particular points of the notch cross-section of N-B specimen, for consecutive blows.
Strain gauge: N° 1, 2, 3, 4, 5 and 12.

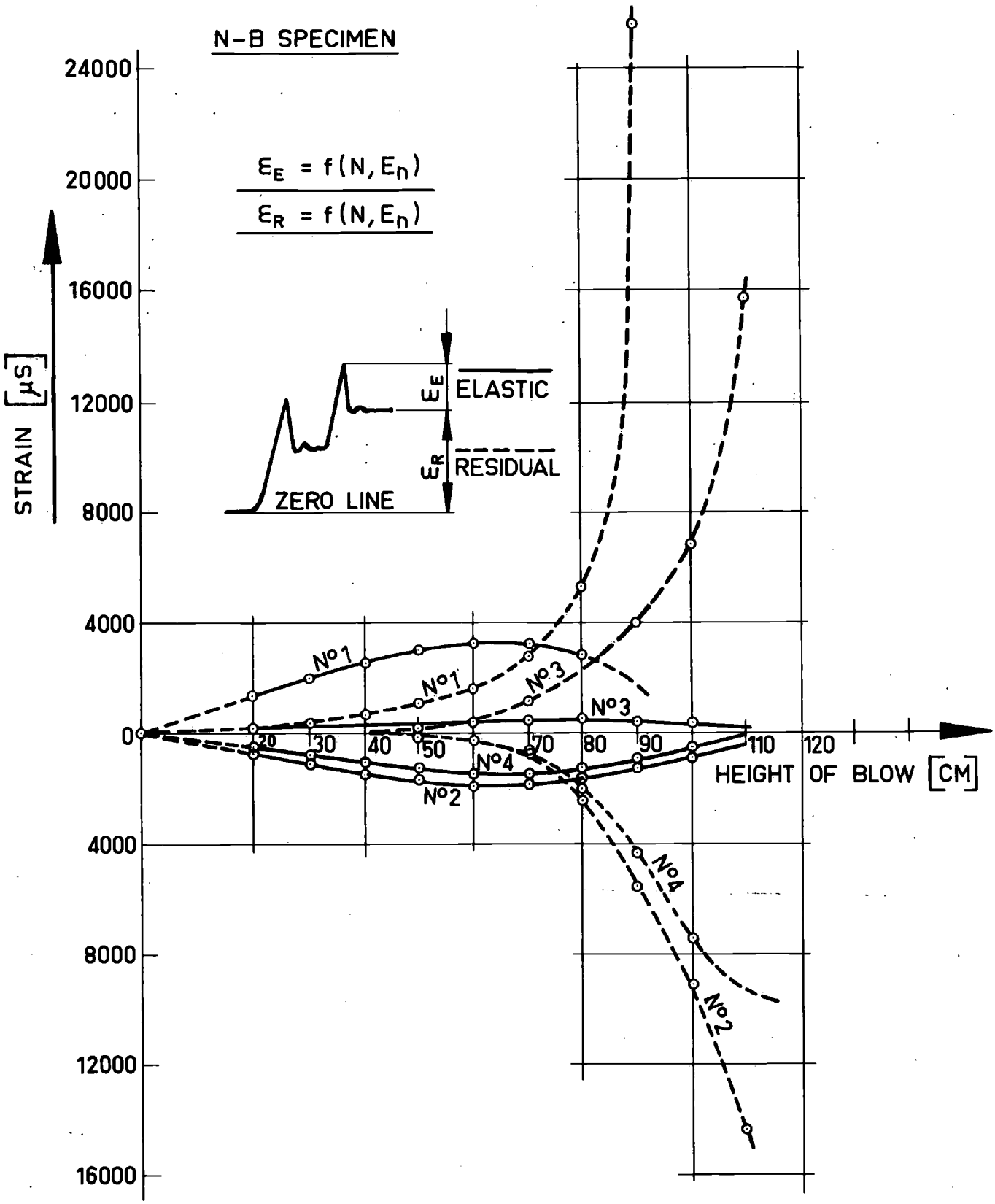

FIG. 10. Magnitude of the elastic strain (ε_E) and residual strain (ε_R) in particular points of the notch cross-section of N-B specimen for consecutive blows.
Strain gauges: Nº 1, 2, 3, 4.

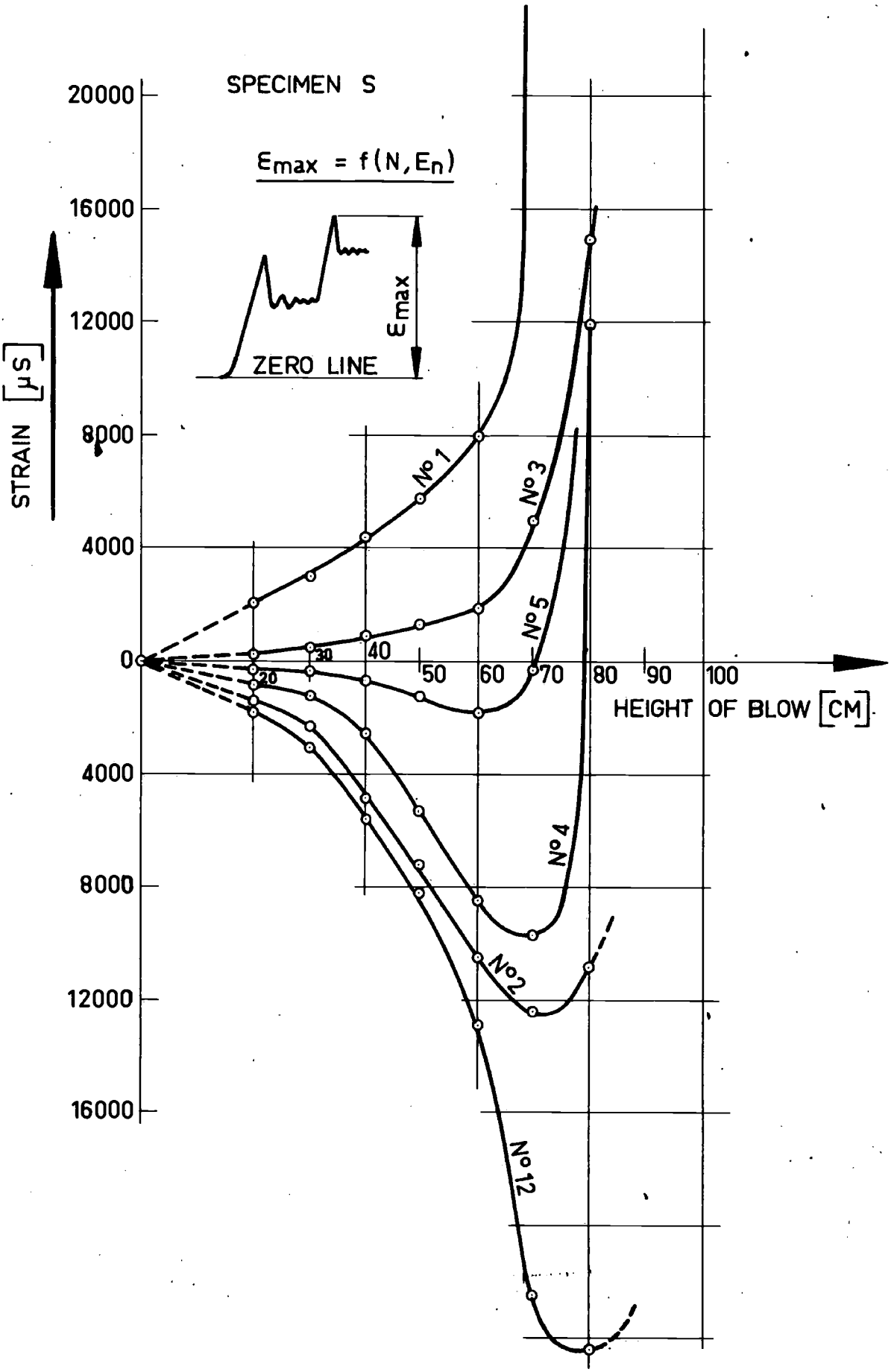

FIG. 9. Maximum strains in particular points of the notch cross-section of S specimen, for consecutive blows. Strain gauges N° 1, 2, 3, 4, 5 and 12.

SPECIMEN S

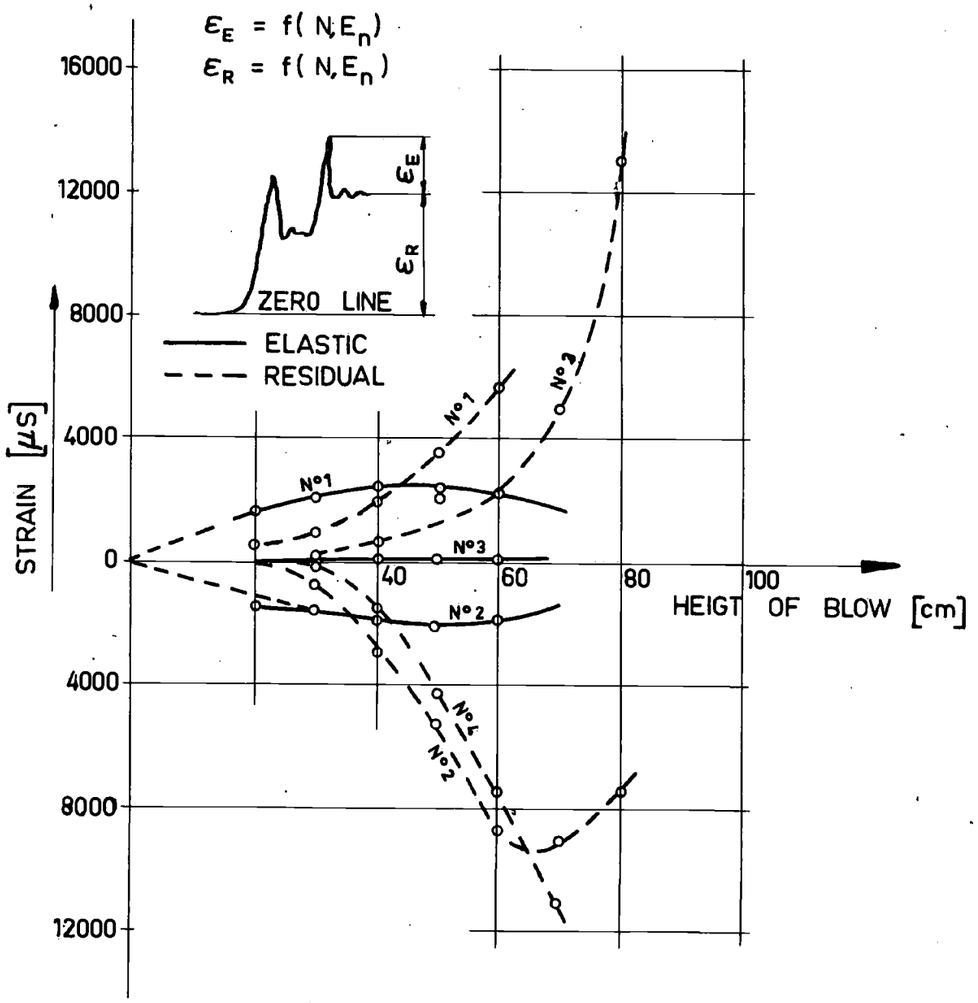

FIG. 11. Magnitude of the elastic strain (ε_E) and residual strain (ε_R) in particular points of the notch cross-section, S specimen, for consecutive blows. Strain gauges: N° 1,2,3,4

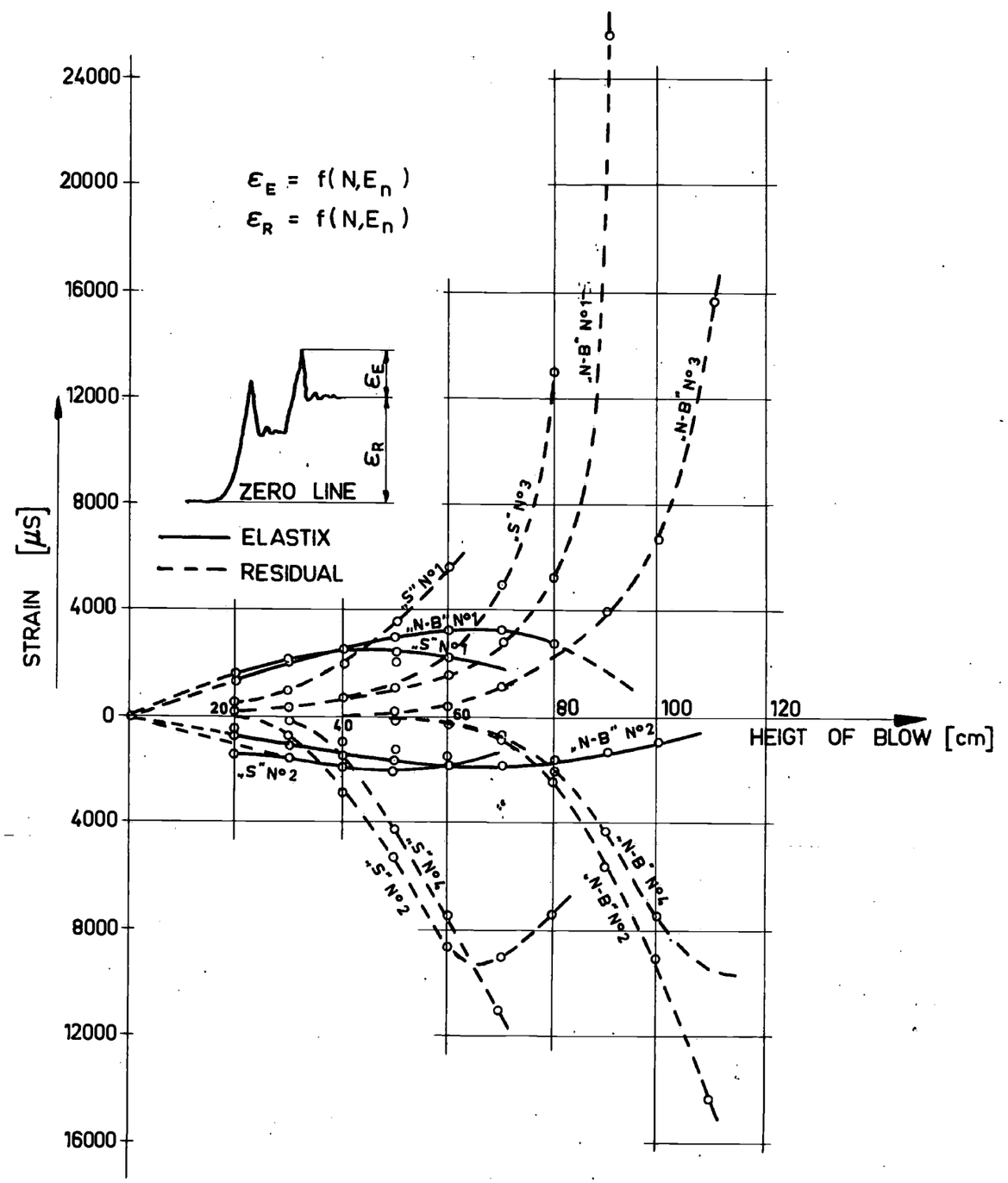

FIG. 12. Comparison of the magnitude the elastic strain (ε_E) and residual strain (ε_R) in particular points of the notch cross-section, N-B and S specimen, for consecutive blows.

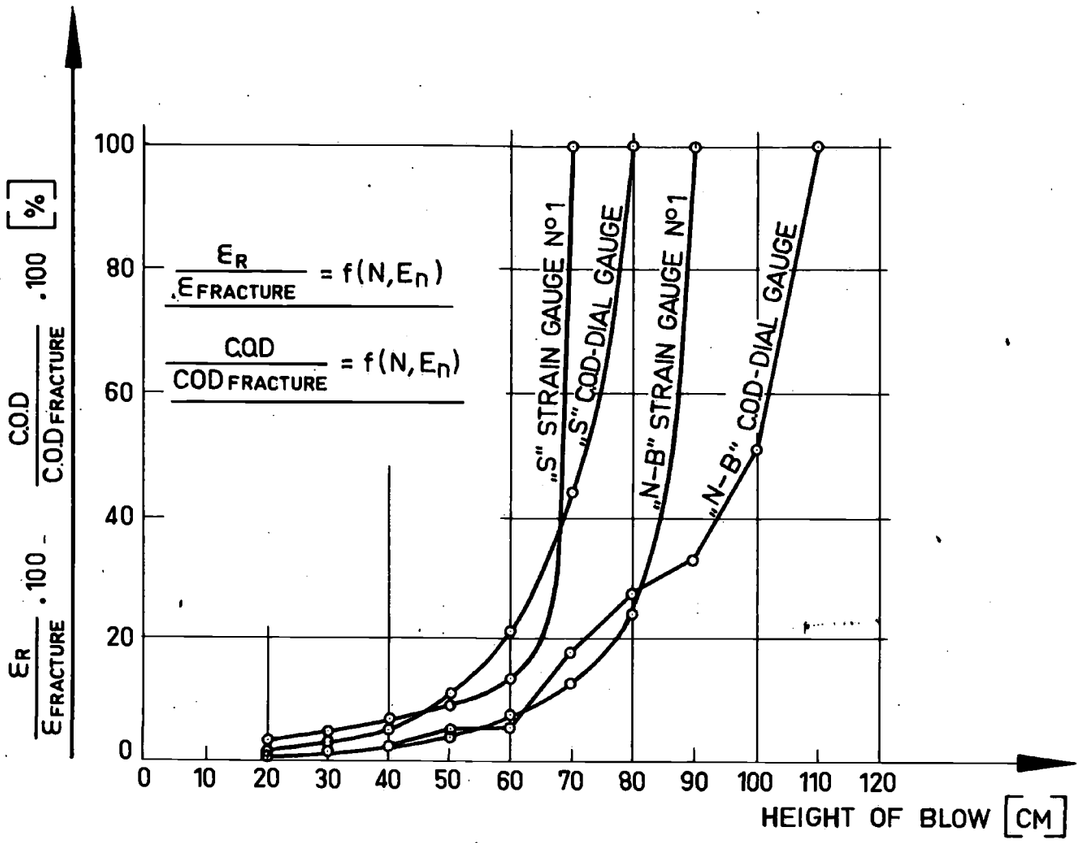

FIG. 13. Comparison of the relative magnitude of residure strain (strain gauge N° 1 in vicinity of the notch) and relative magnitude of COD (measured by means of COD-dial gauge) for consecutive blows, for the N-B and S specimen.

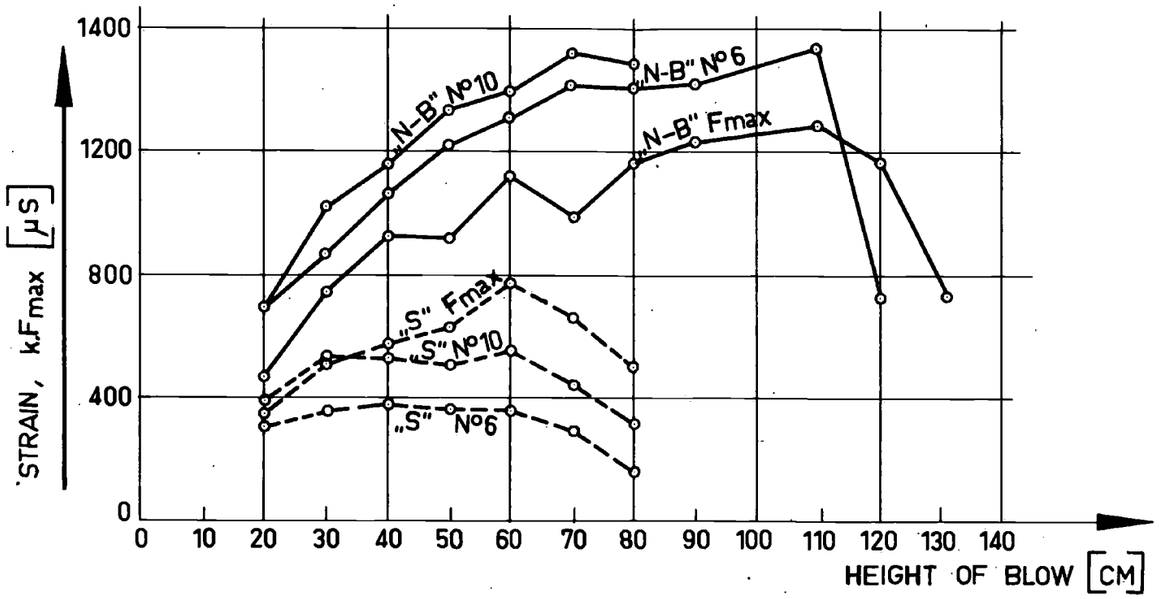

FIG. 14. Magnitude of strain indicated by the strain gauge N° 6 and 10 for consecutive blows in relation to the maximum impact force (F max) for specimen N-B and S.

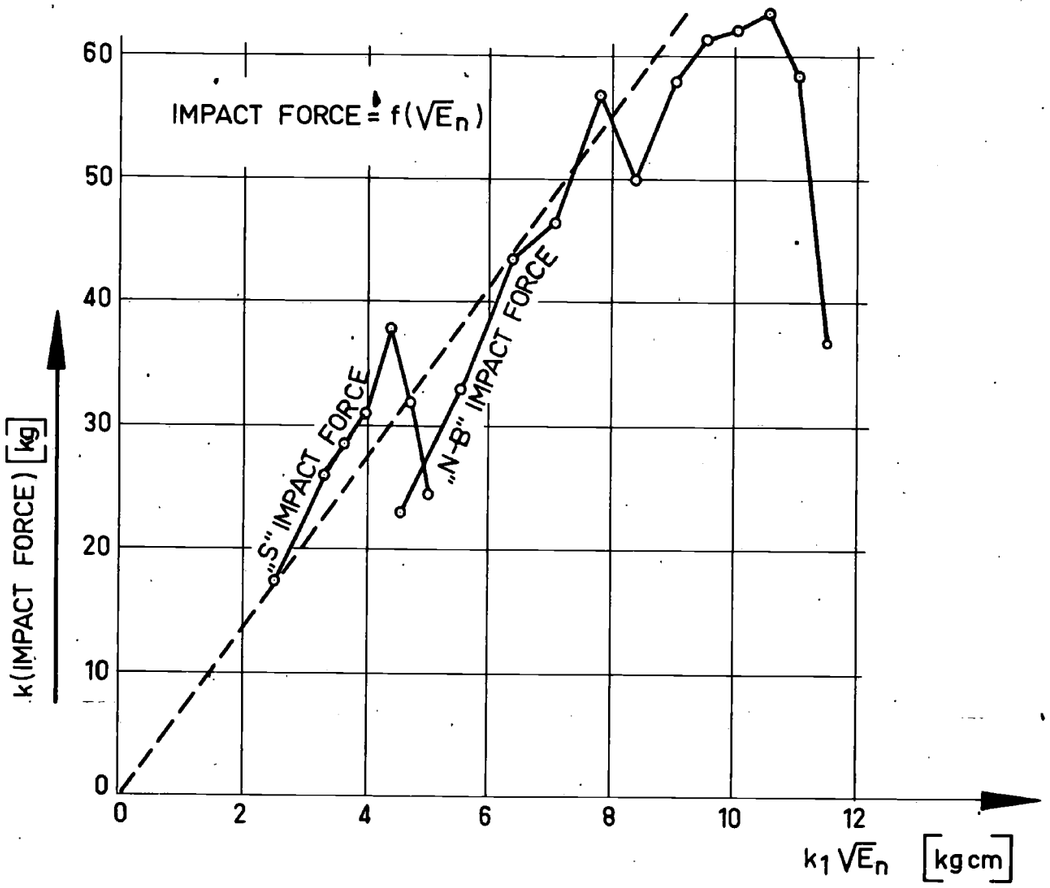

FIG. 15 Comparison of the impact force for consecutive blows for specimens N–B and S, as function of $\sqrt{E_n}$.

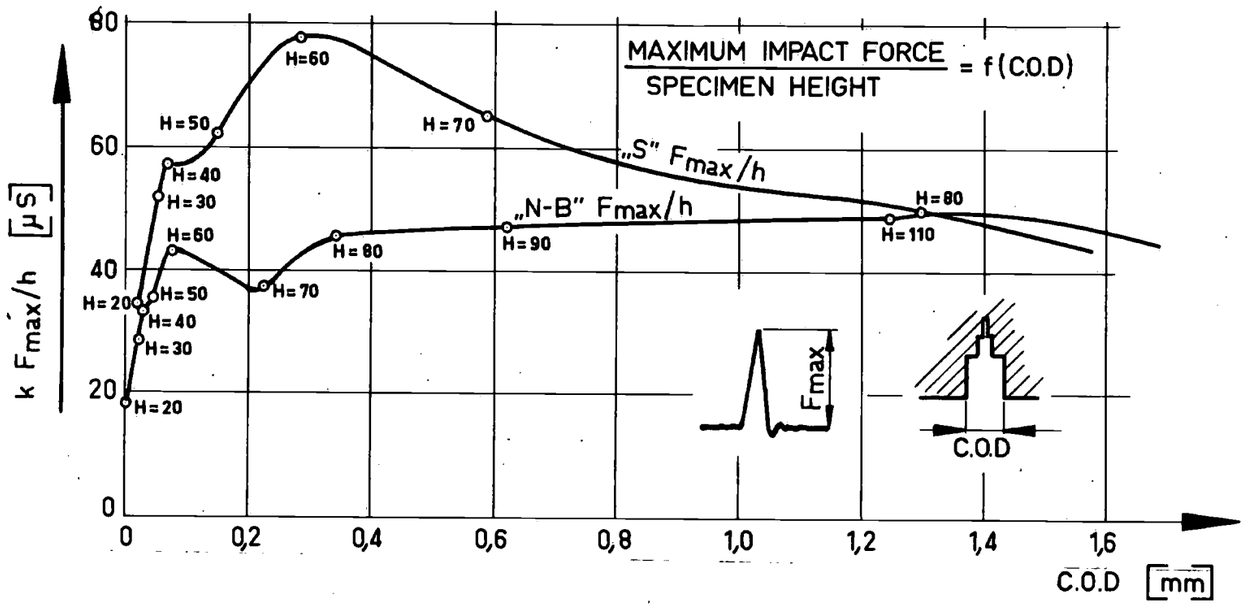

FIG. 16 Maximum impact force Fmax. (in relation to specimen height) measured on the bridge part, as function of the C.O.D.–values measured after blow, by means of C.O.D.–dial gauge. Comparison for specimens N–B and S.

FIG 15/R 2

FIG 16 R/2

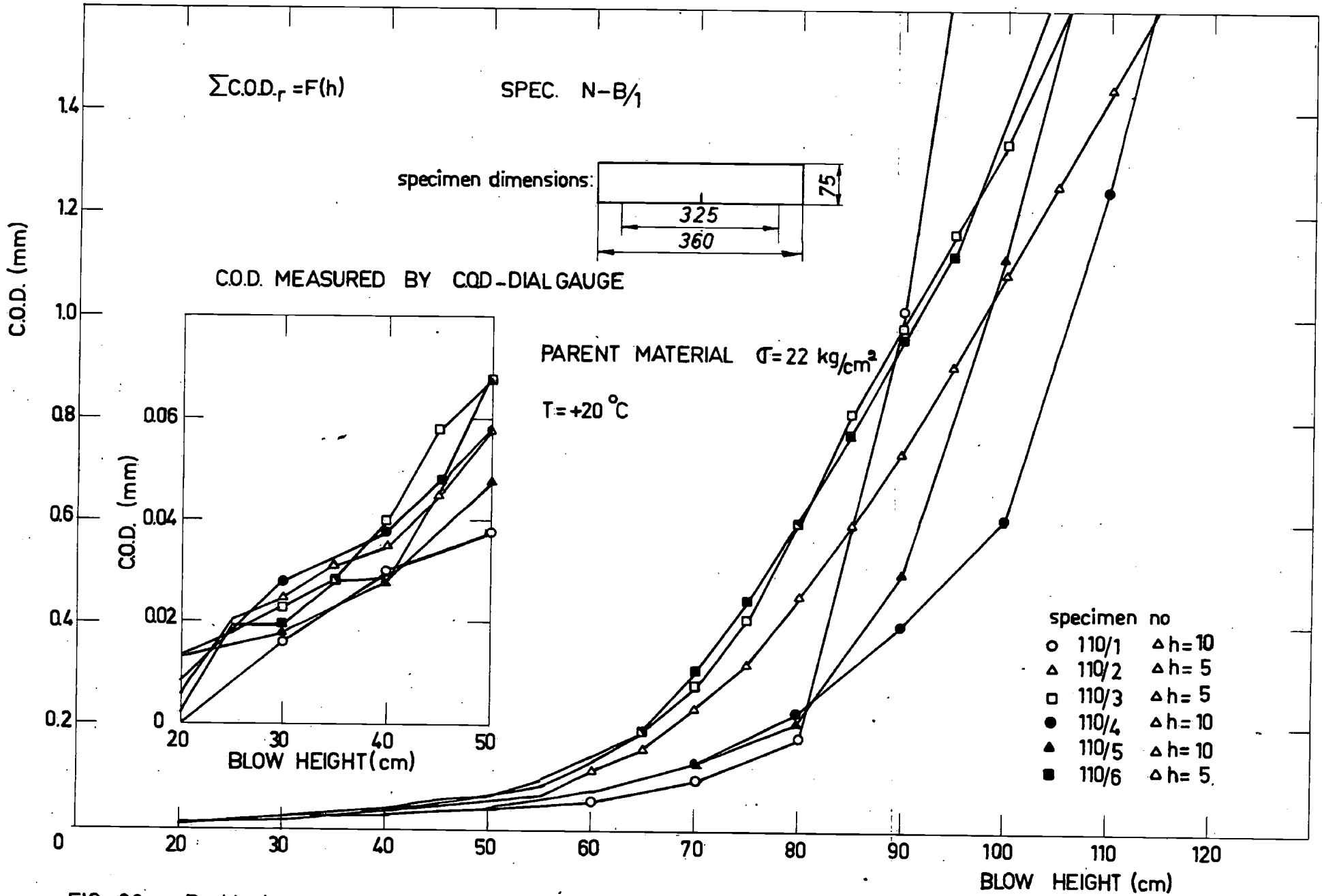

FIG. 20. Residual value of the COD as function of the height of the blow. Results for the NIBLINK tests specimens, tested at temperature T = + 20 °C.

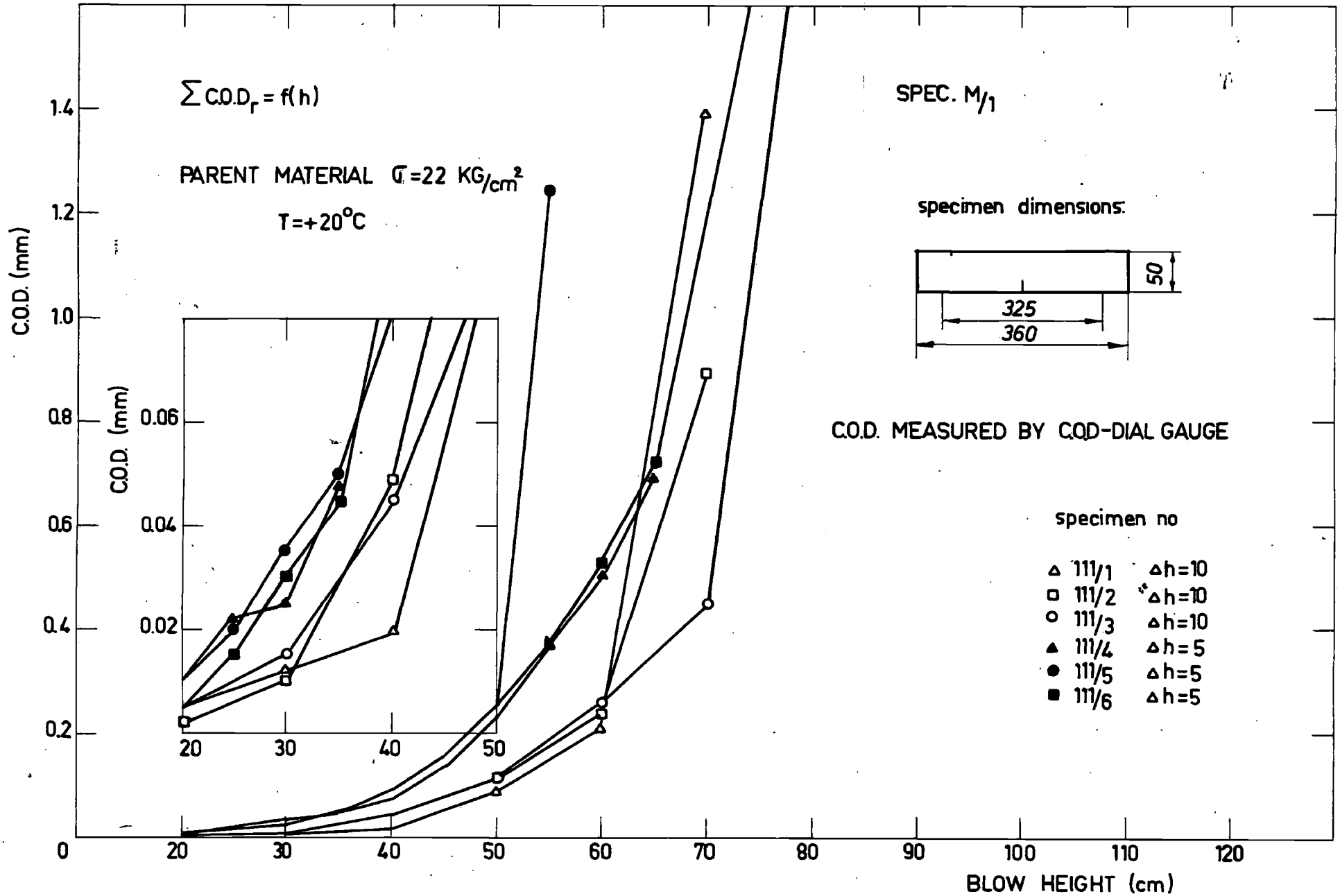

FIG. 21. Residual value of the COD as function of the height of the blow. Results for the specimens series 1, group M/1, tested at temperature T = + 20 °C.

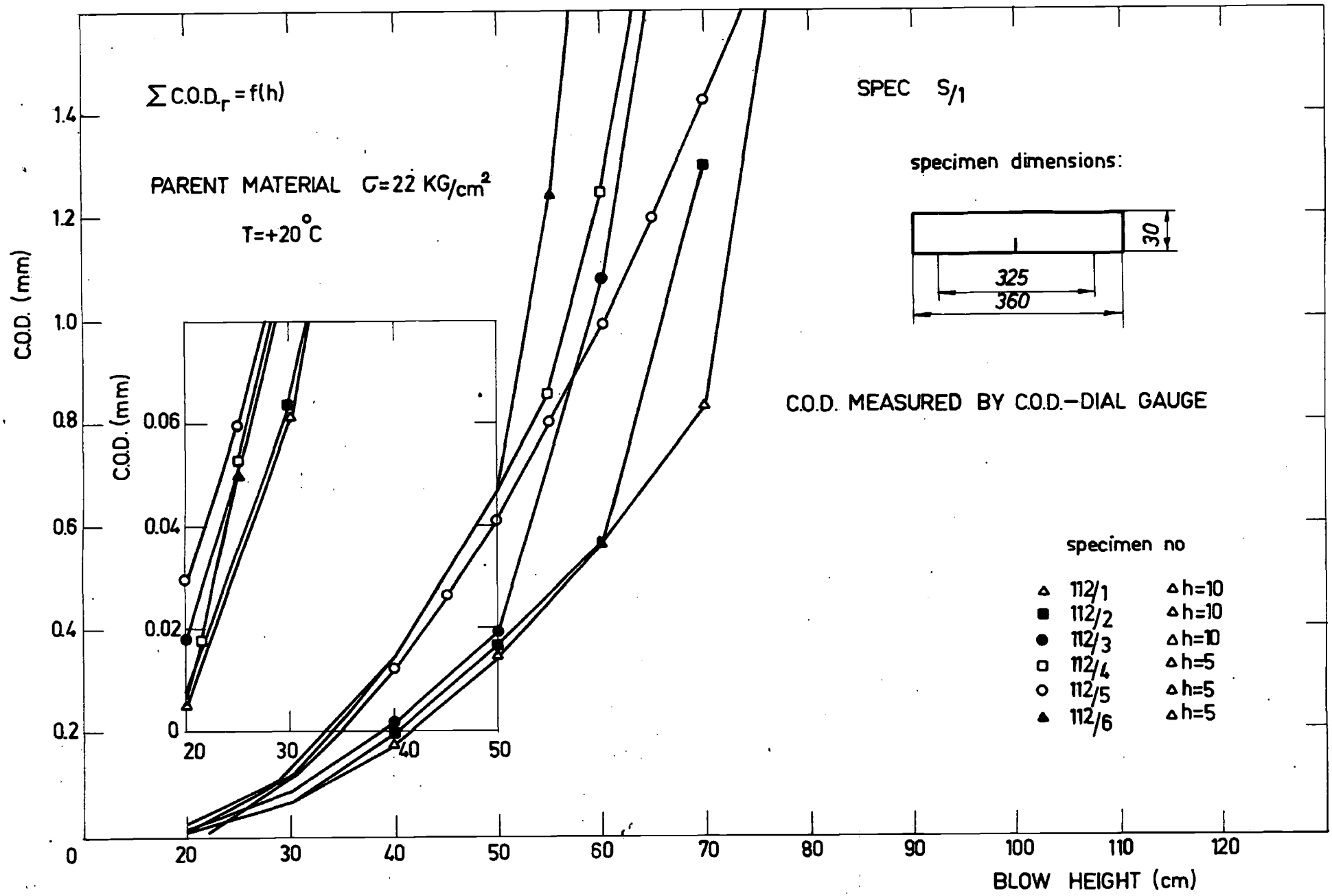

FIG. 22 Residual value of the C.O.D. as function of the height of the blow.
Resuls for the specimens series 1, group S/1, tested at temperature T= +20 °C.

2214

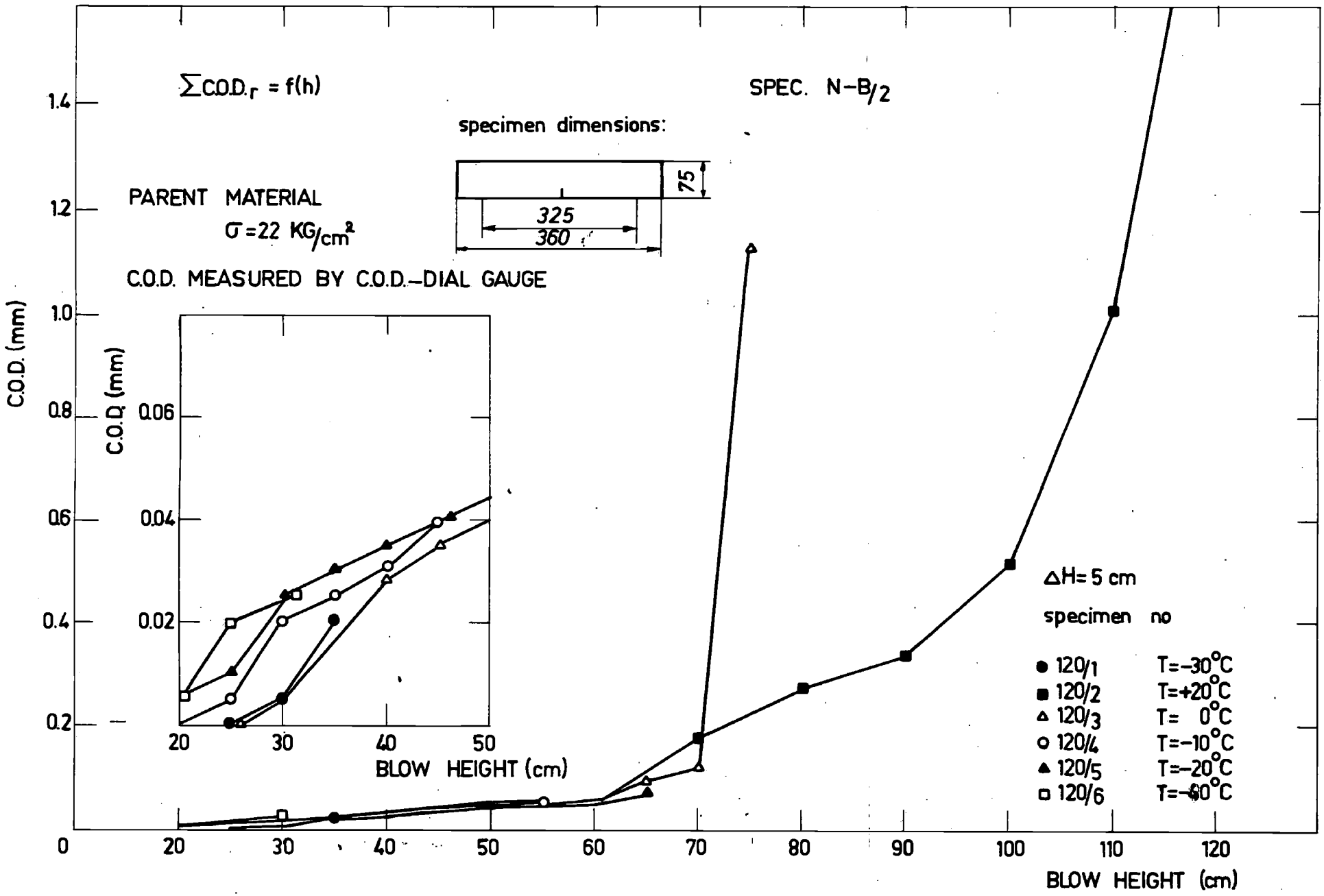

FIG. 23. Residual r-value of the COD as function of the height of the blow. Results for the specimens serres 2, group N-B / 2, tested at temperatures T = + 20 ° ; 0 °; - 20° and - 40 °C.

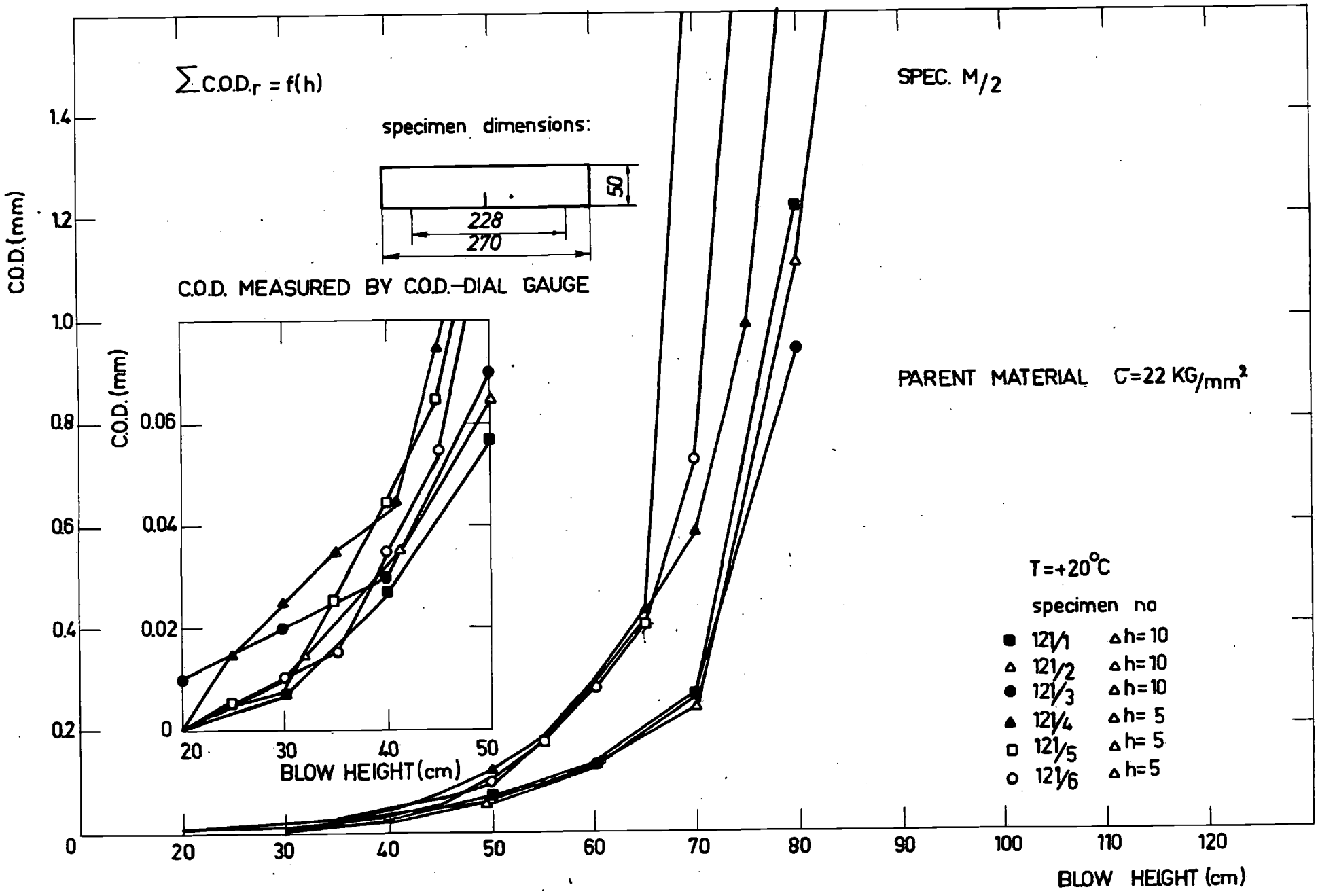

FIG. 24 Residual value of the C.O.D. as function of the height of the blows.
Results for the specimens series 2, group M/2, tests at temperature T= +20 °C.

122

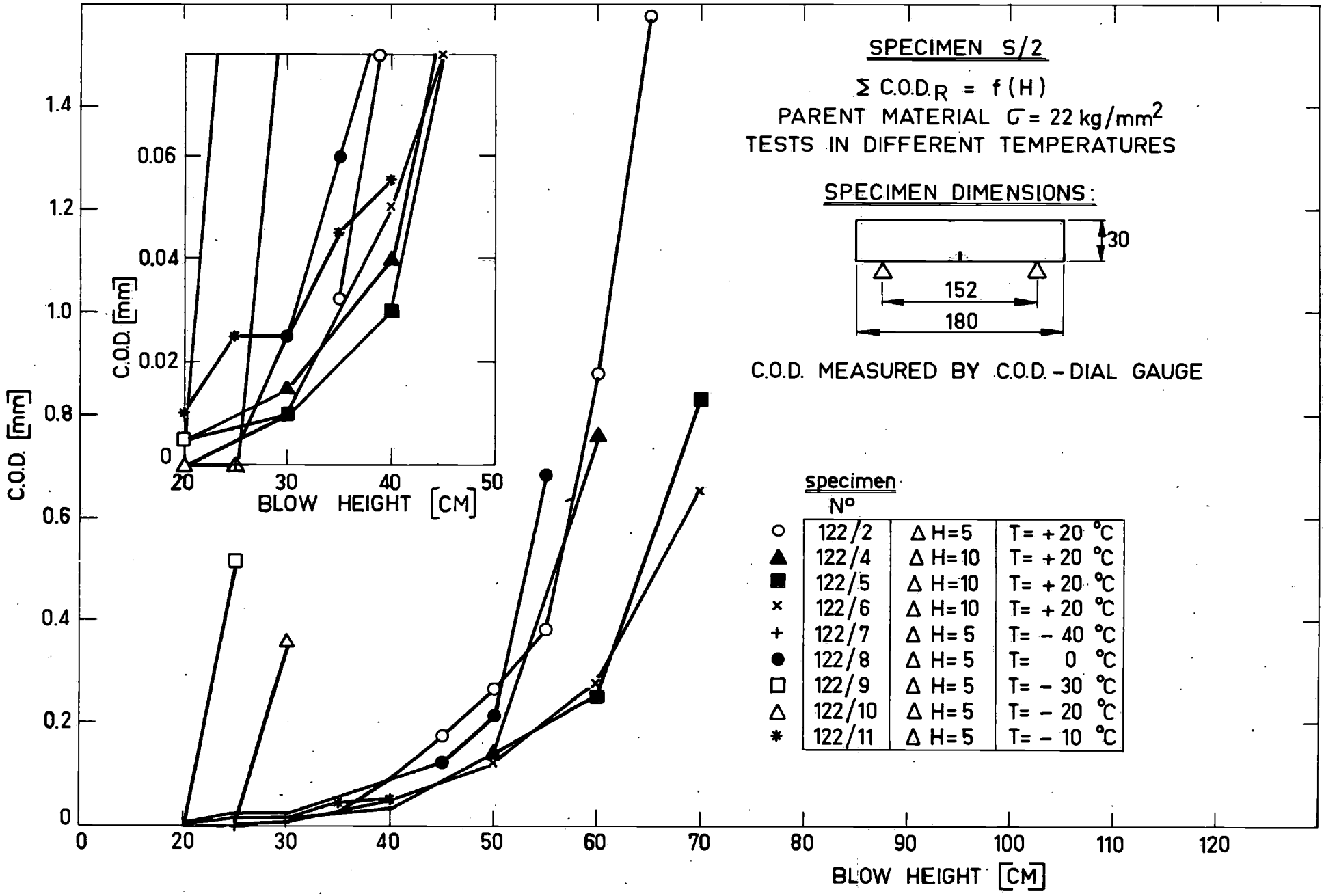

FIG. 25. Residual value of the COD as functie of the height of the blow. Results for the specimens serres 2, group S/2, tested at temperature T = +20°; 0°; – 20° and 40°C.

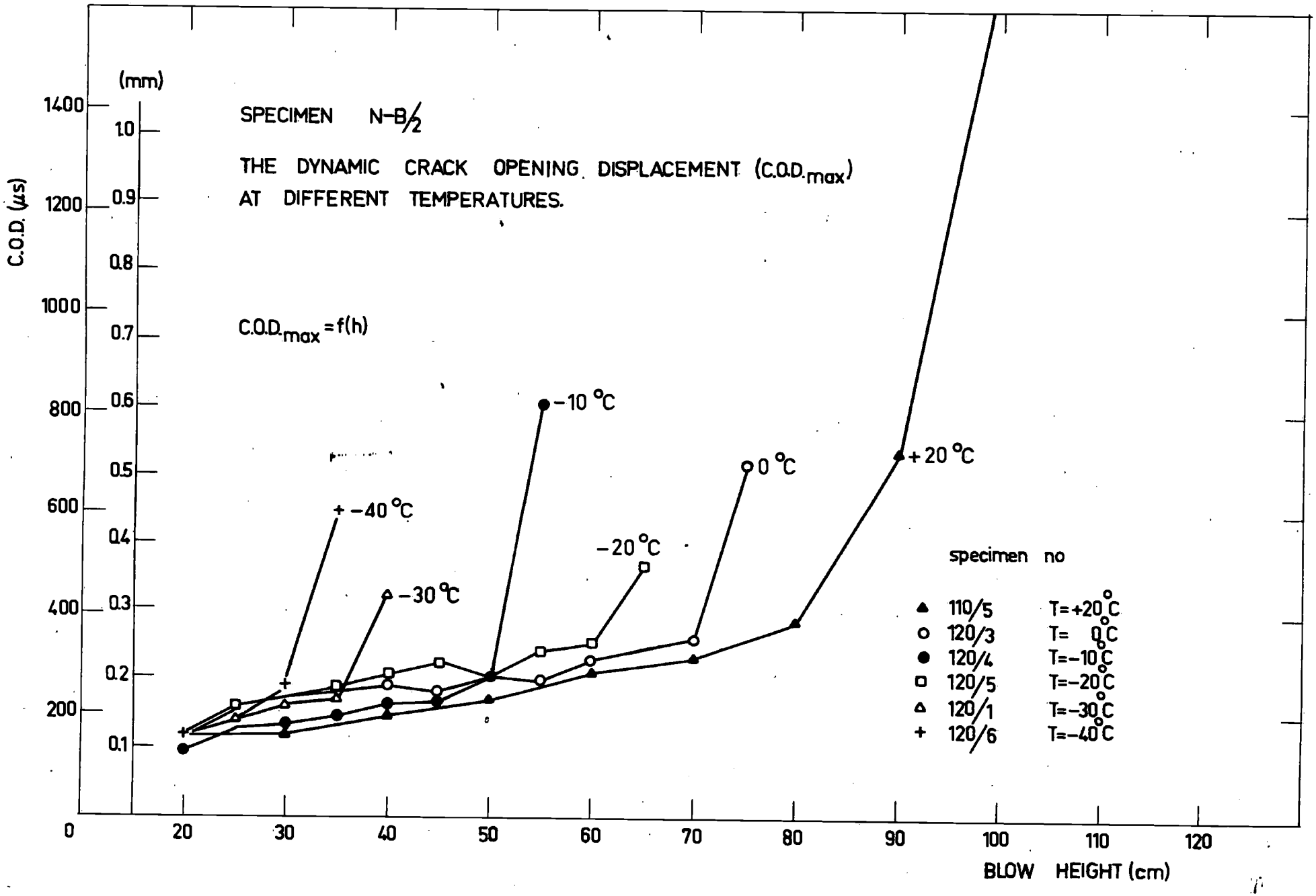

FIG. 26 The dynamic crack opening displacement (C.O.D.max.) as function of the height of the blow. Results for the series 2, group N-B/2, tested at temperatures T= +20°; 0°; -10°; -20°; -30° and -40 °C.

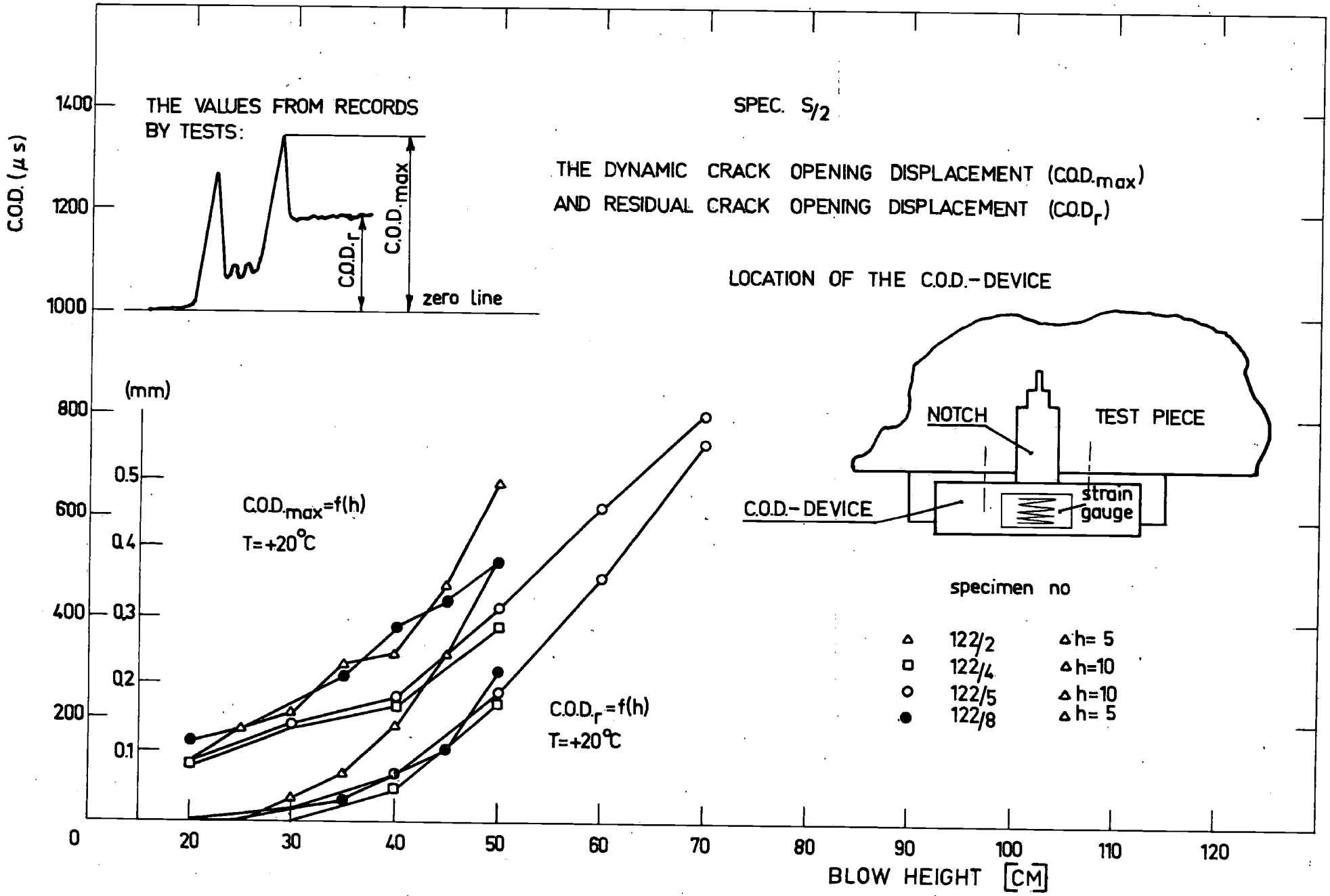

FIG. 27 The dynamic crack opening displacement (C.O.D. max.) and residual crack opening displacement (C.O.D. r) as function of the height of the blow.
Results for the series 2, group S/2, tested at temperature T= +20 °C.

FIG 27 /2

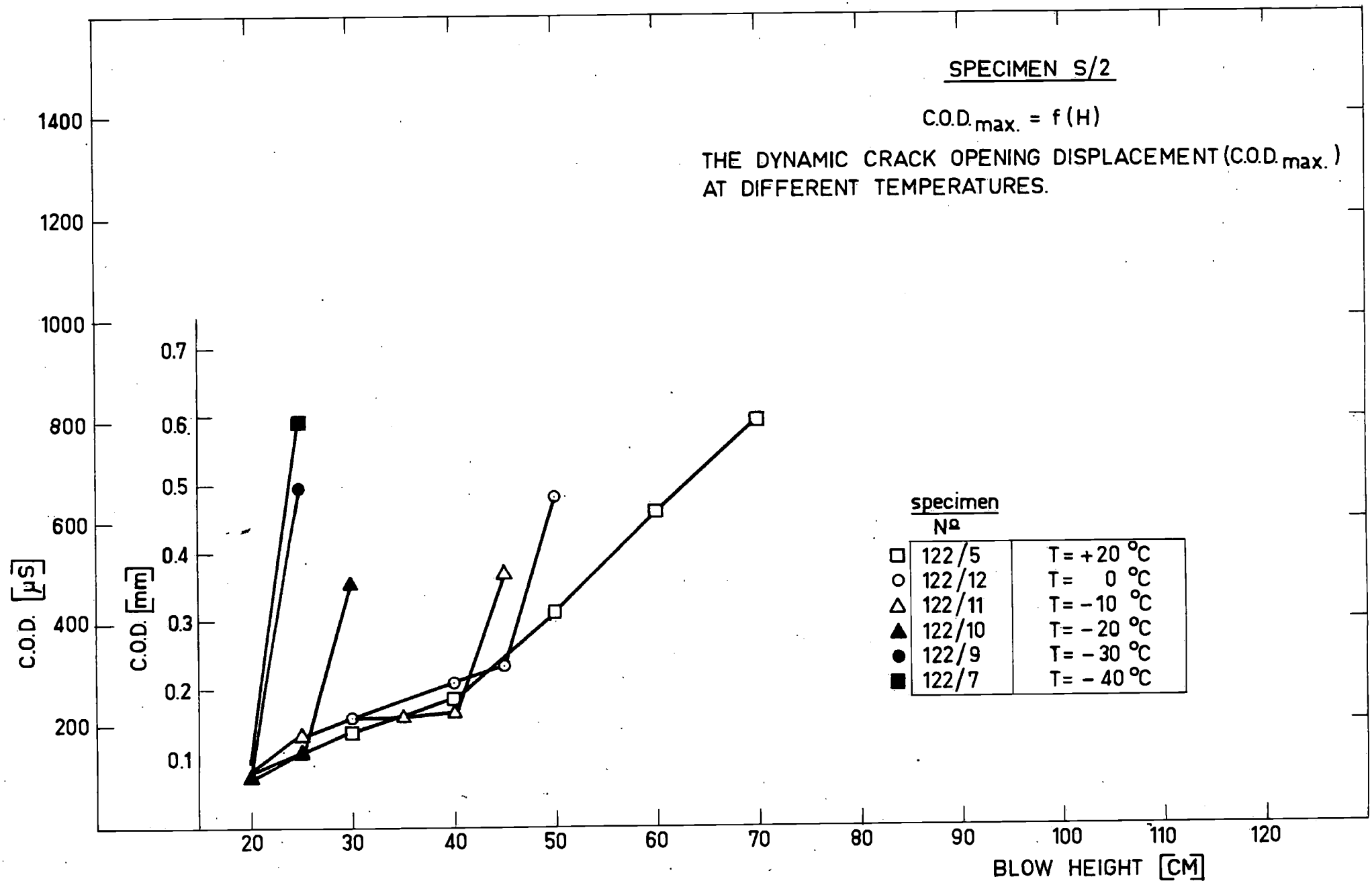

FIG. 28. The dynamic crack opening displacement (COD max) as function of the height of blow. Results for the series 2, group S/2, tested at temperatures T = +20°; 0° ; -10° ; -20° ; -30°; and 40 °C.

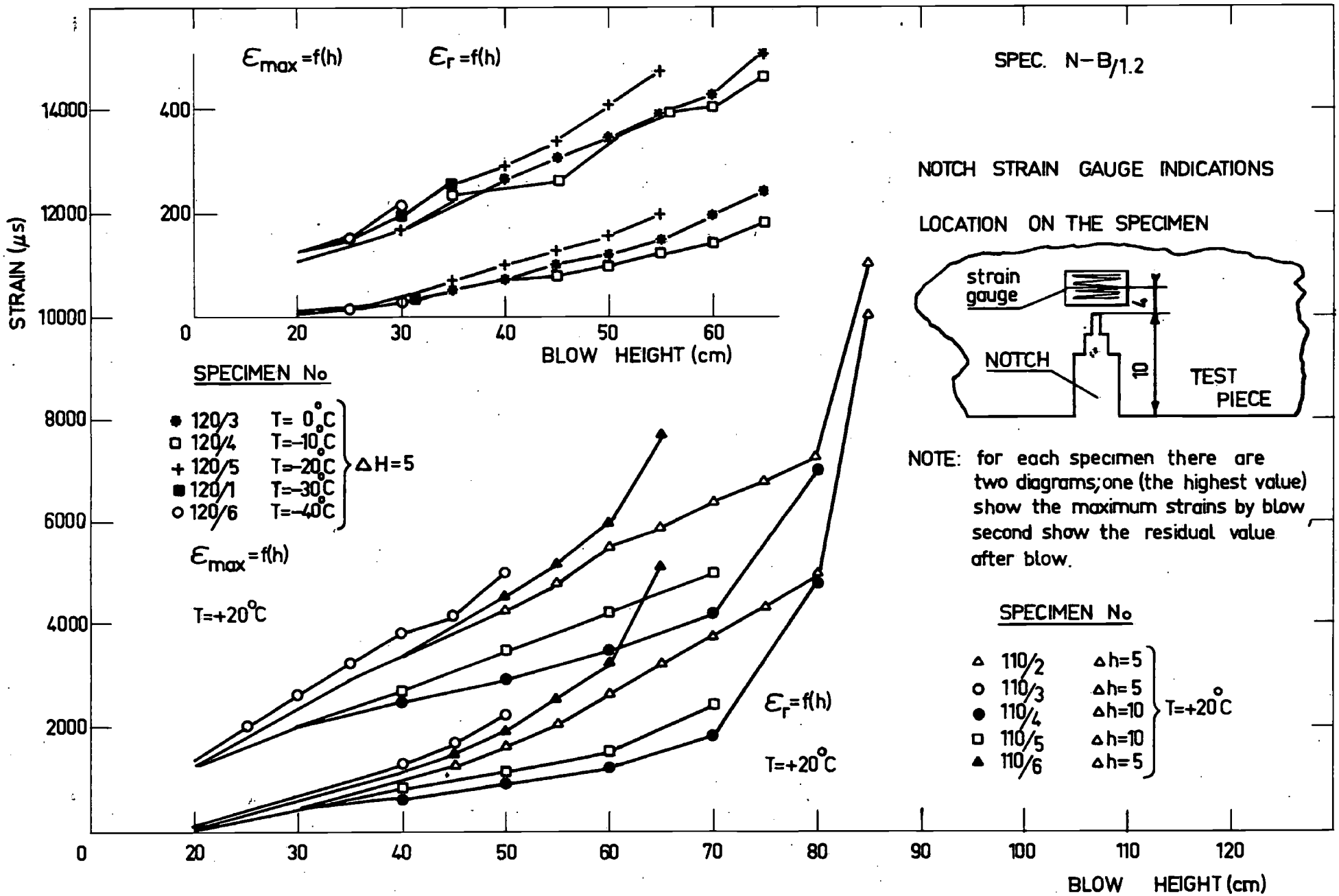

FIG. 29. Maximum (Emax) and residual (ε_r) strains in the region of the notch. Results for the specimens serres 1 and 2, NIBLINK type.

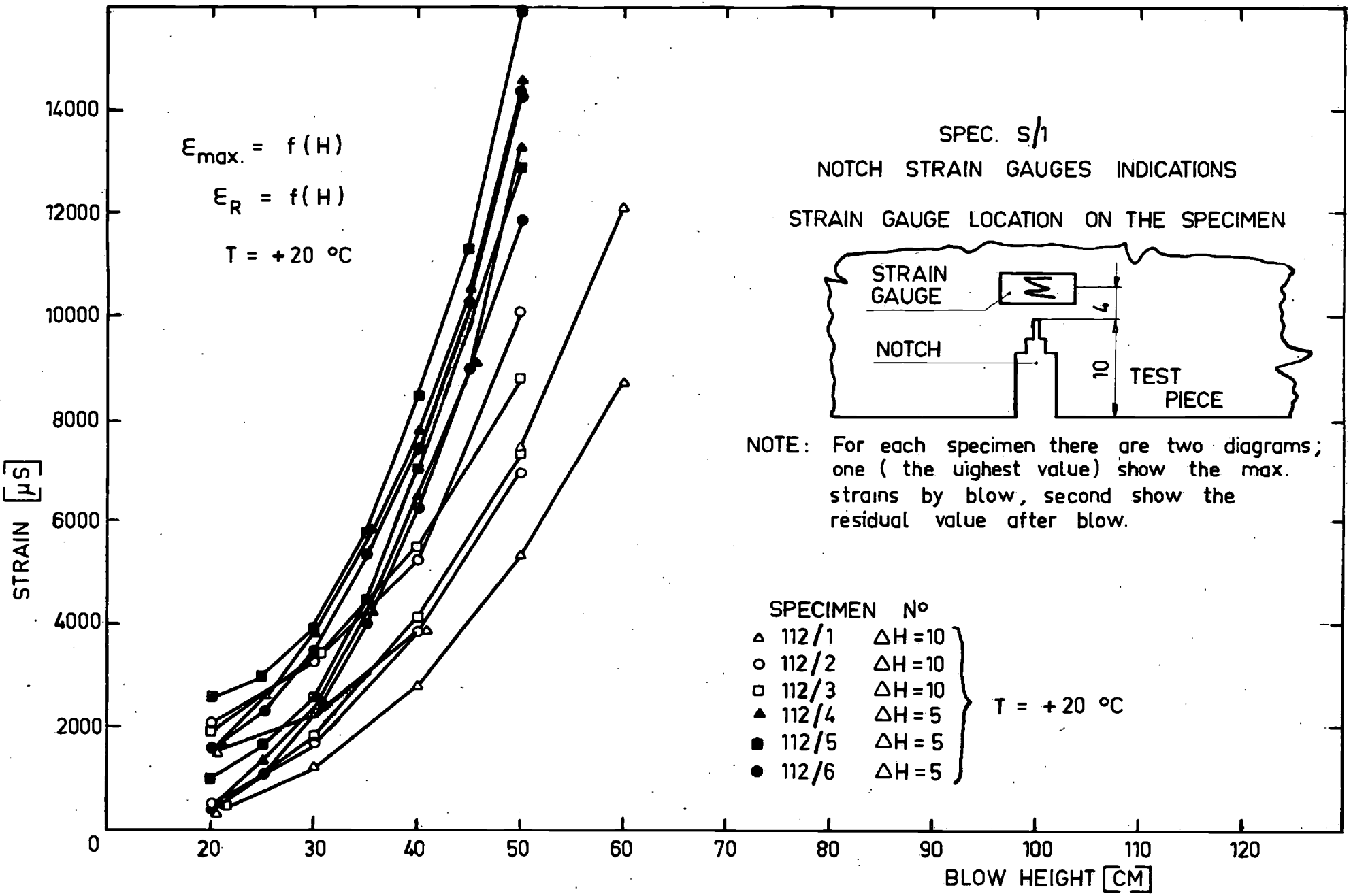

FIG. 30. Strains in the region of the notch. Results for the specimens series 1, S/1 type.

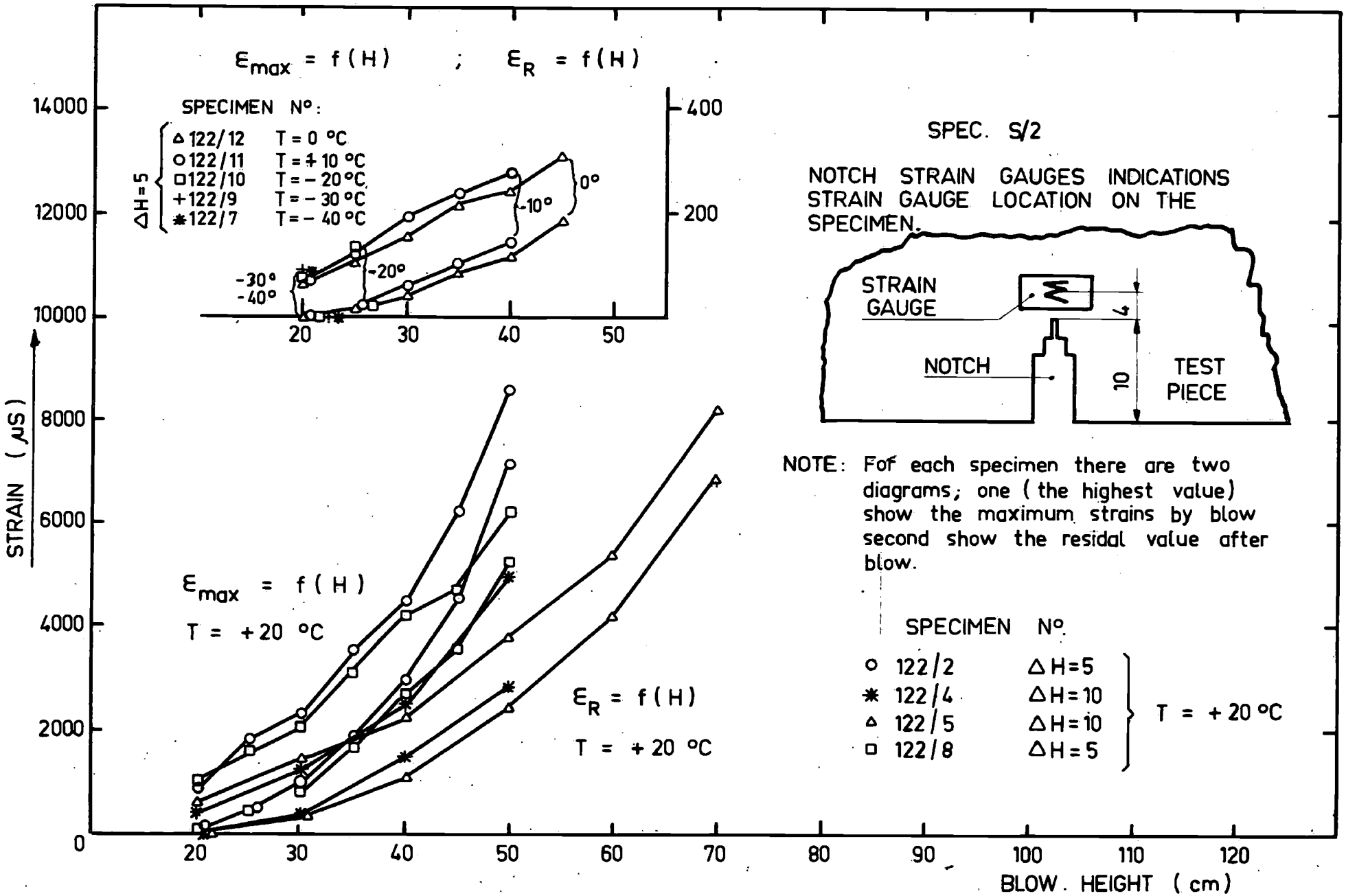

FIG. 31. Maximum (ε max) and resudual (εr) strain in the region of the notch. Results for the specimens series 2, S/2 type.

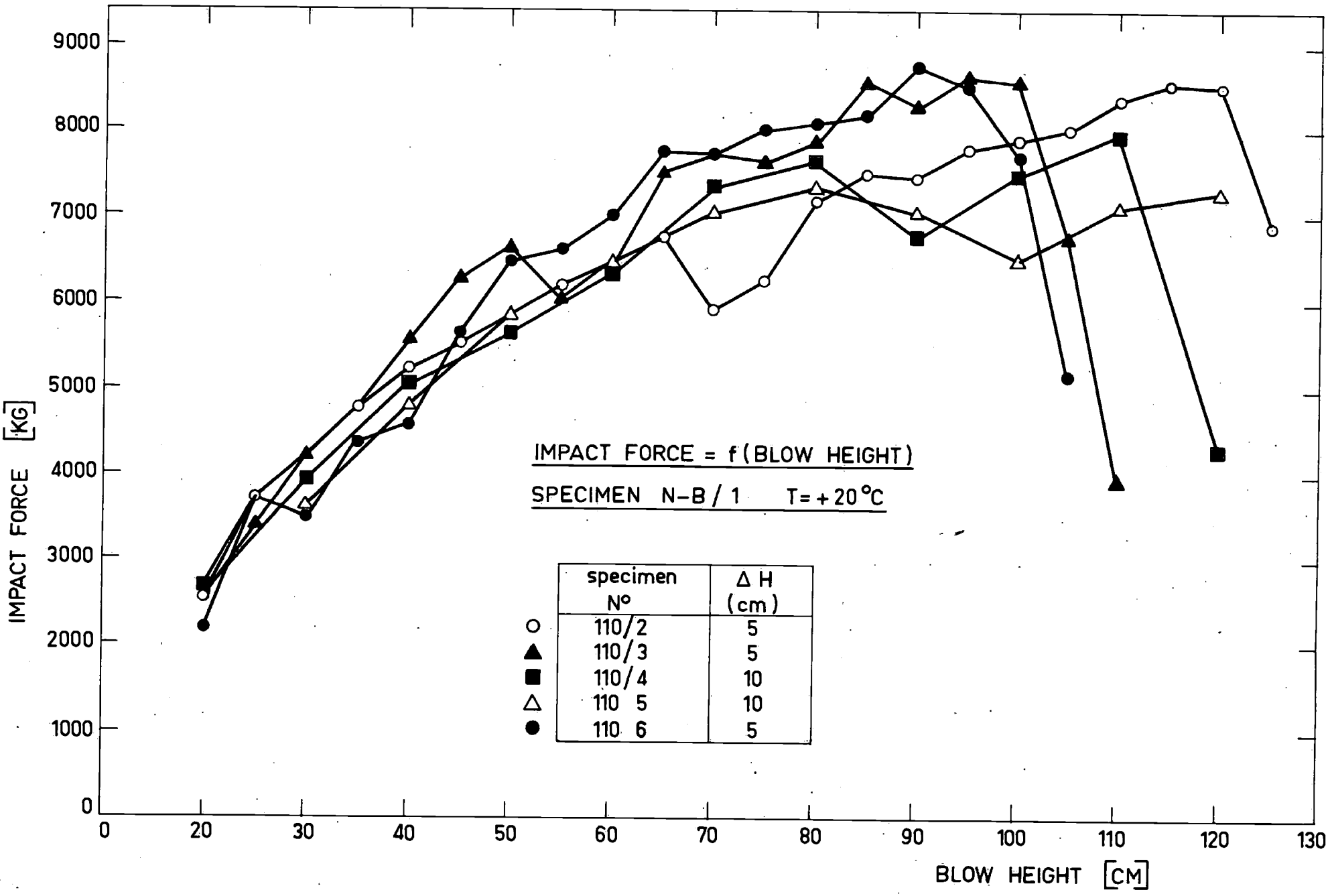

FIG. 32 Impact force as function of the height of the blow. Results for the specimens series 1, group N-B/1 (NIBLINK) tested at temperature T= + 20 °C.

Fig 32 /E

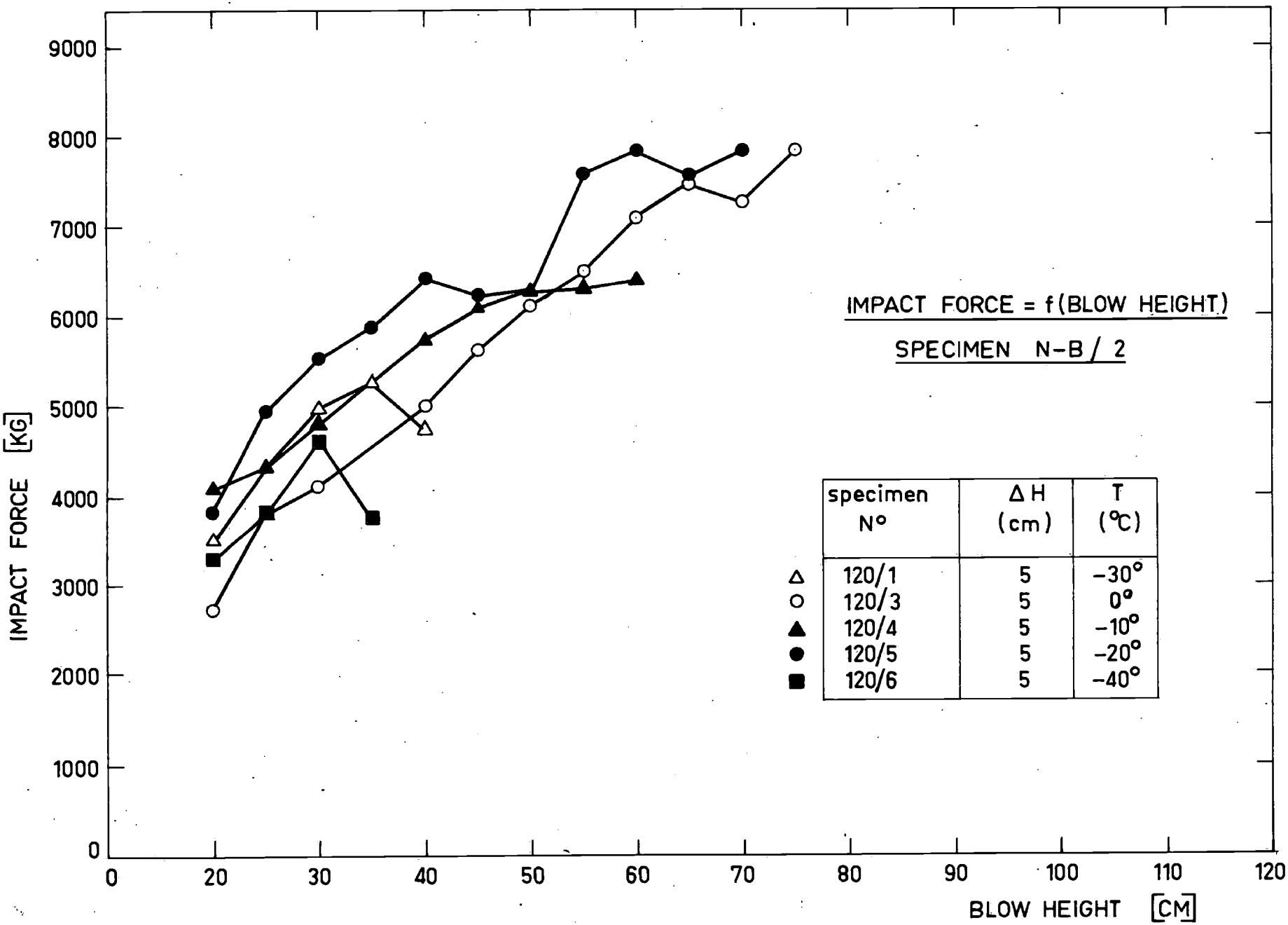

FIG. 33. Impact force as function of the height of the blow. Results for the specimens series 2, group N-B / 2 (NIBLINK), tested at temperatures T = 0°, -10°, -20°, -30° and -40°.

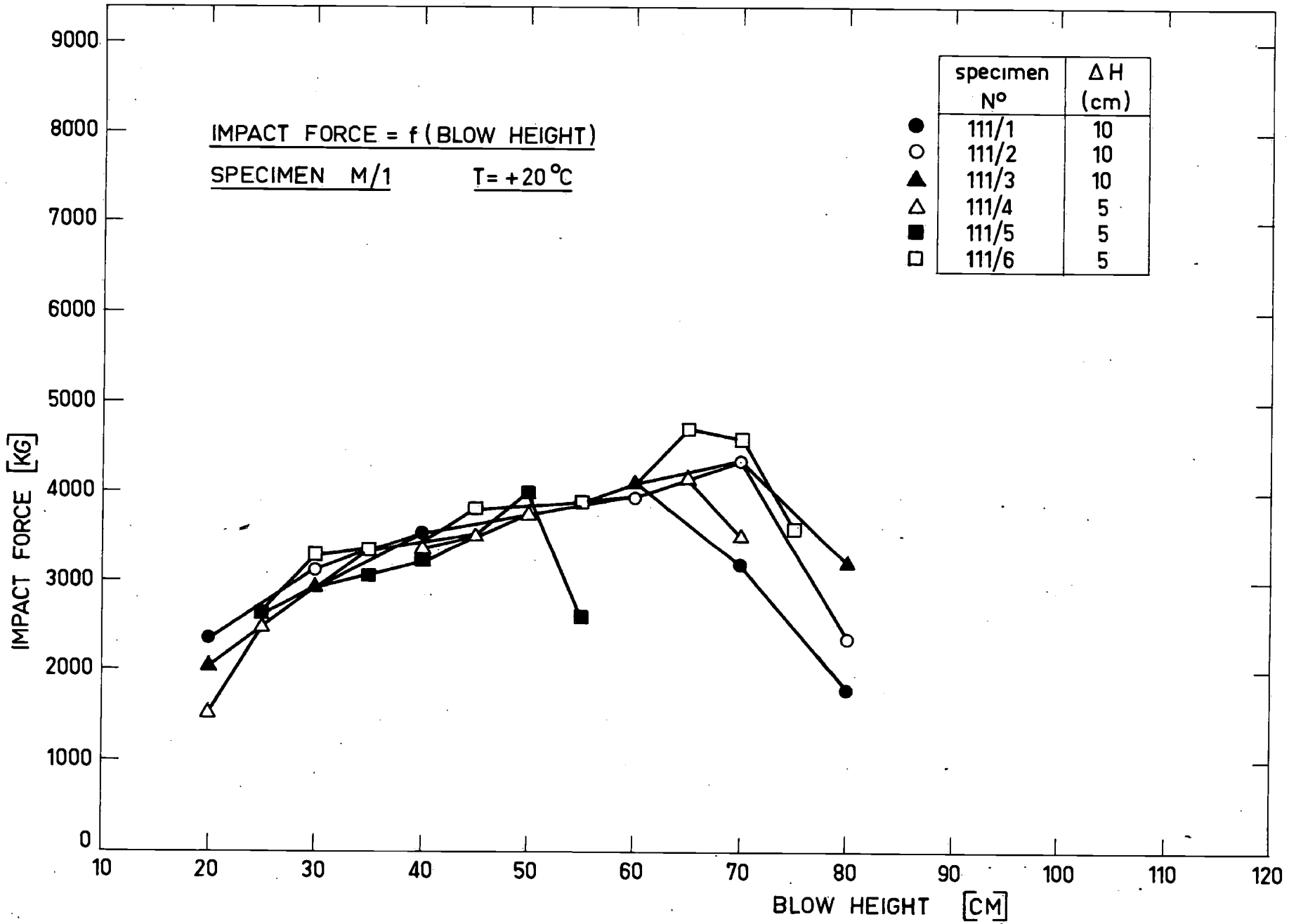

FIG. 34 Impact force as function of the height of the blow. Results for the specimens series 1, group M/1, tested at temperature T= +20 °C.

FIG 34/E2

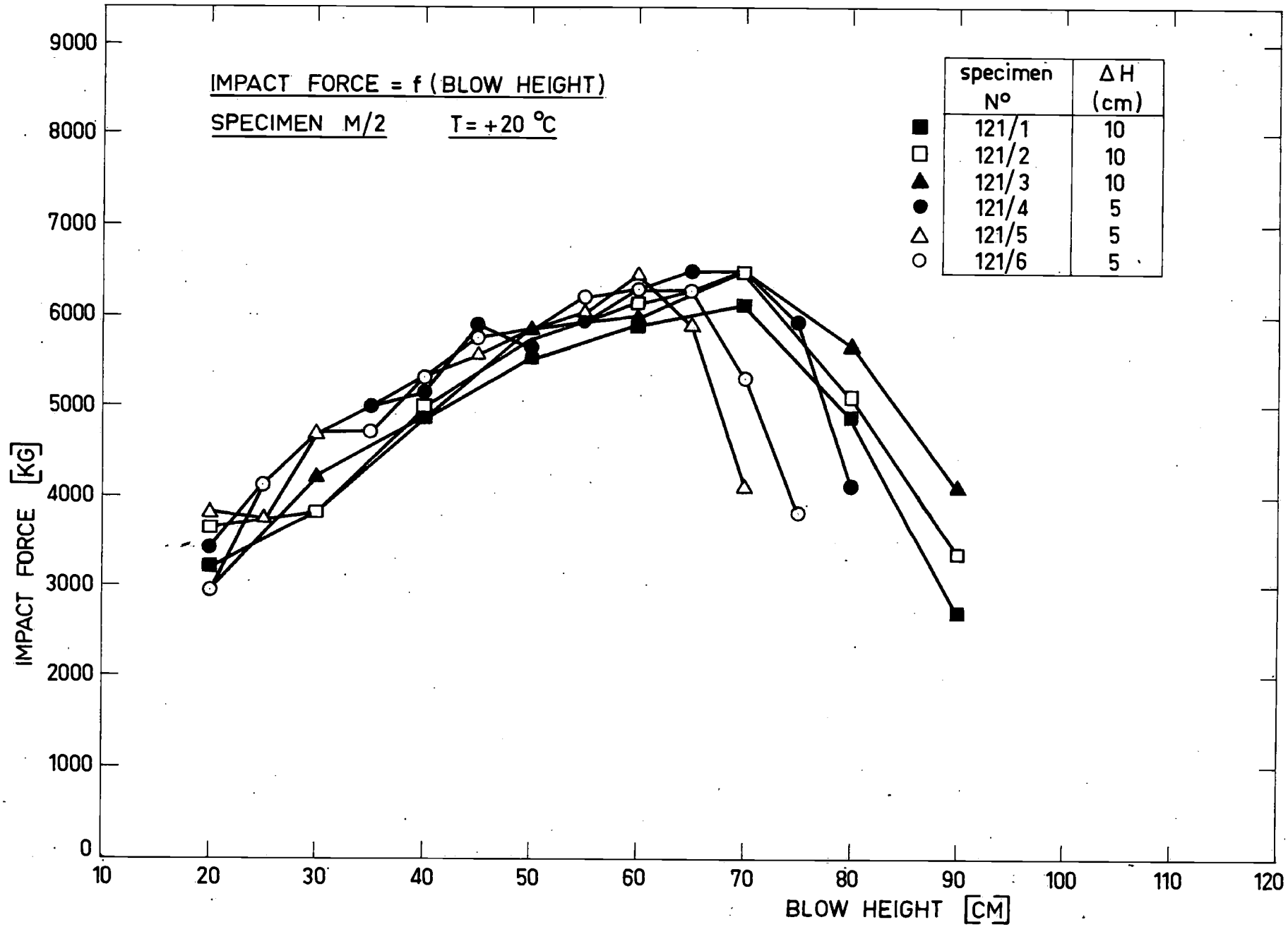

FIG. 35 Impact force as function of the height of the blow. Results for the specimens series 2, group M/2, tested at temperature T = +20 °C.

FIG 35/M 2

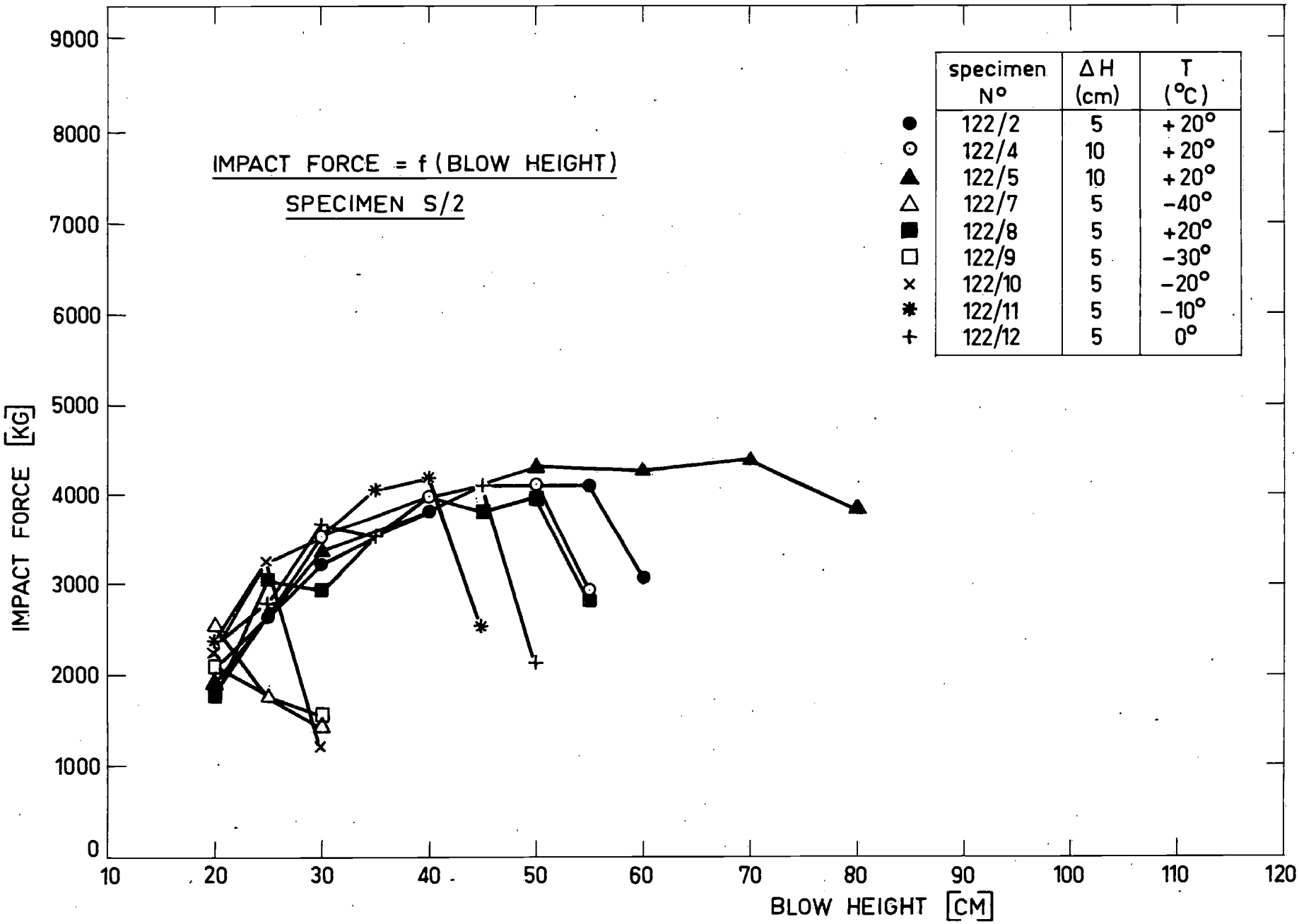

FIG. 36. Impact force as function of the height of the blow. Results for the specimens series 2, group S/2, tested at temperatures T = +20°, 0°, -10°, -20°, -30° and -40°.

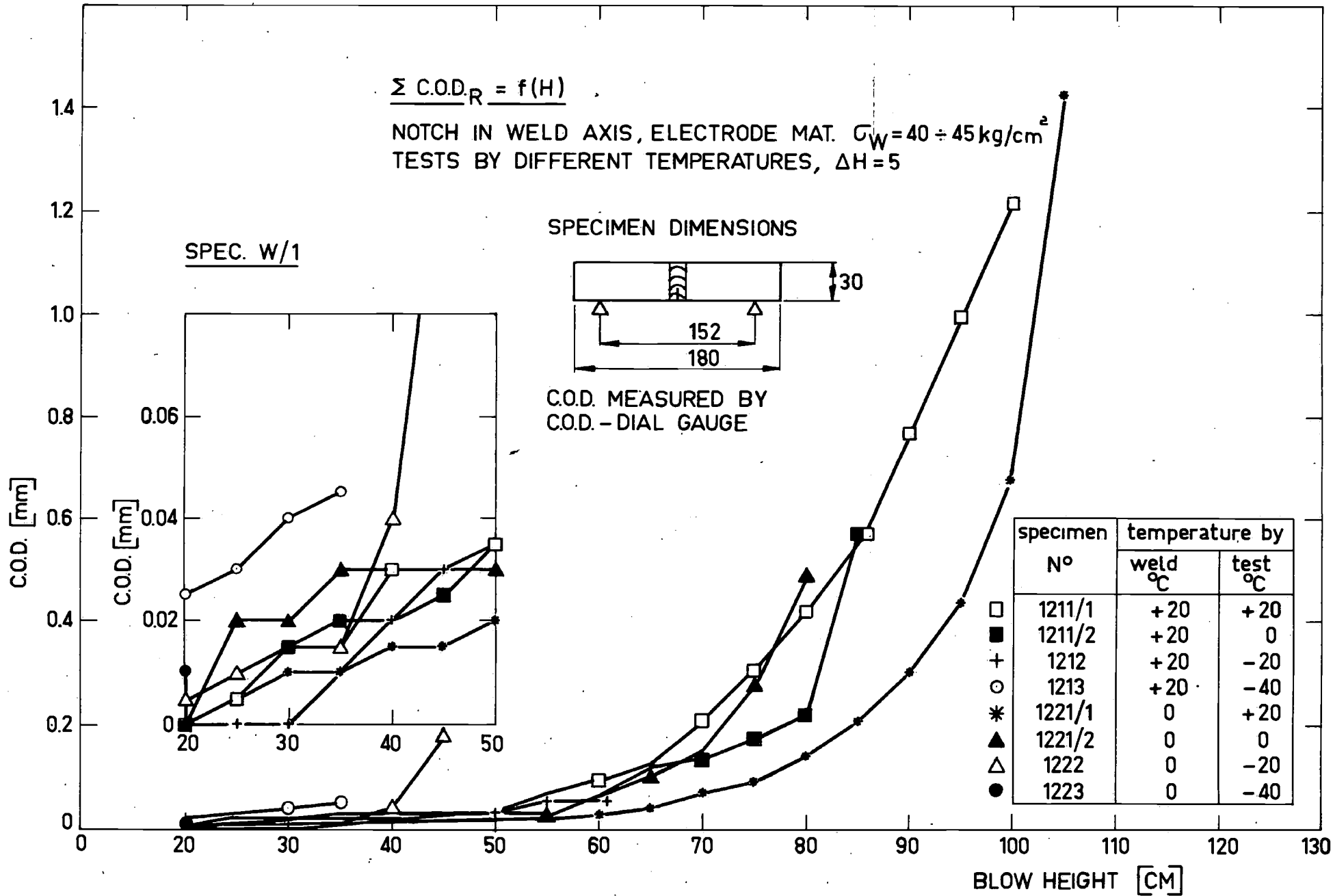

FIG. 38. Residual value of the COD as function of the height of blow. Results of the tests of the welded specimens, group W/1.

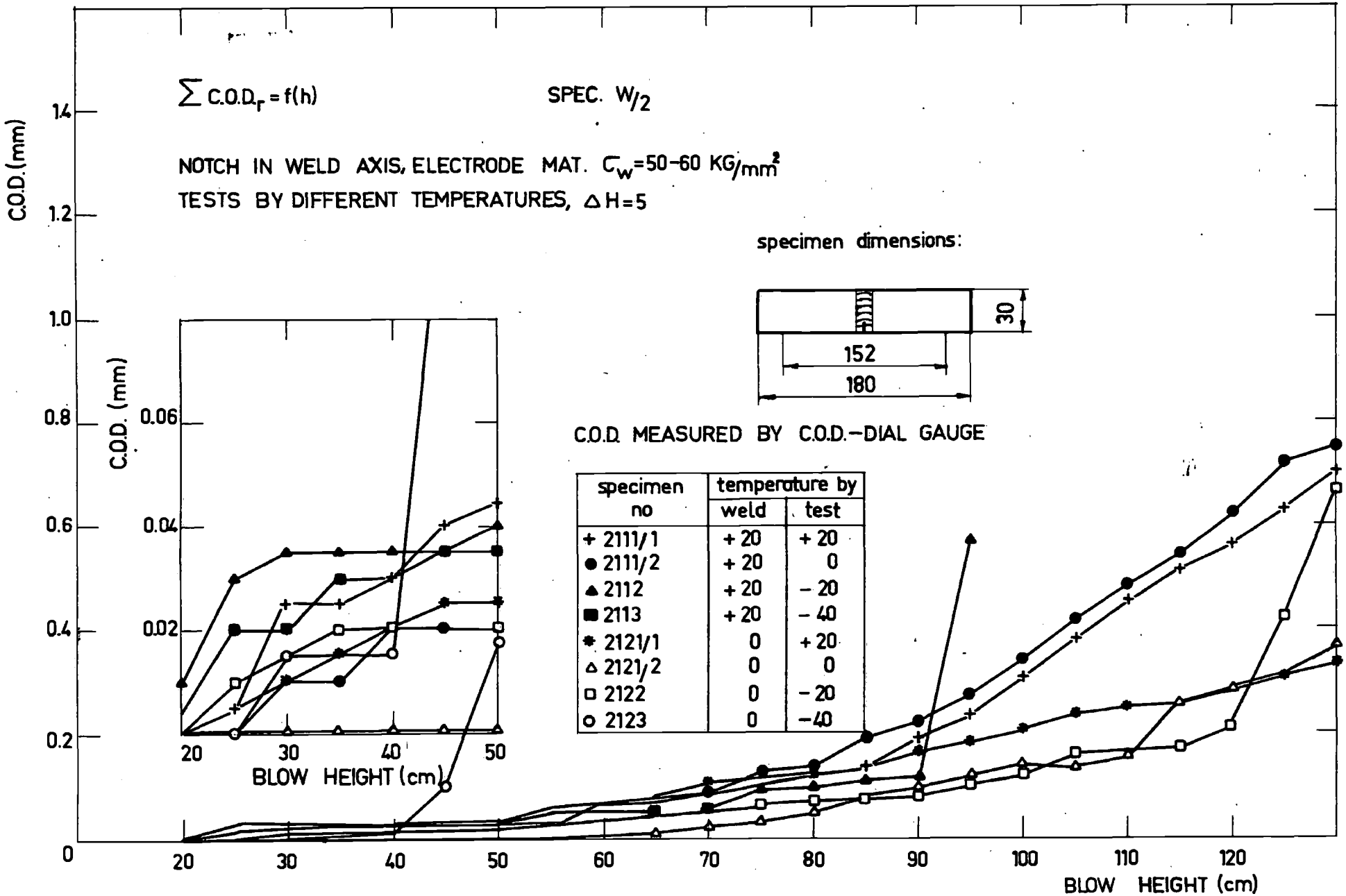

FIG. 39 Residual value of the C.O.D. as function of the height of the blow. Results of the tests of the welded specimens, group W/2

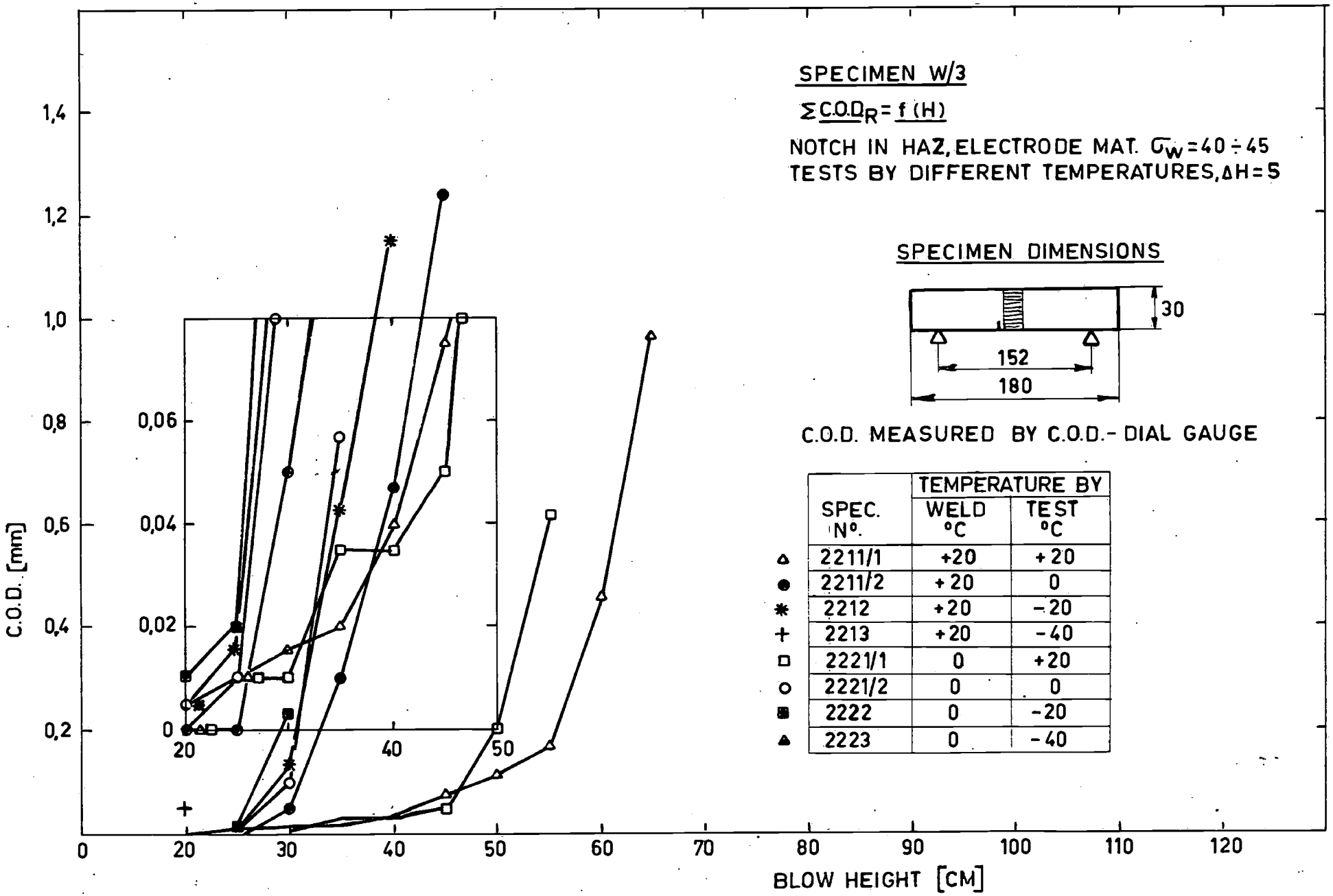

	SPEC. N°.	TEMPERATURE BY WELD °C	TEST °C
△	2211/1	+20	+20
●	2211/2	+20	0
✱	2212	+20	-20
+	2213	+20	-40
□	2221/1	0	+20
○	2221/2	0	0
■	2222	0	-20
▲	2223	0	-40

FIG. 40. Residual value of the COD as function of the height of blow. Results of the tests of the welded specimens group W/3.

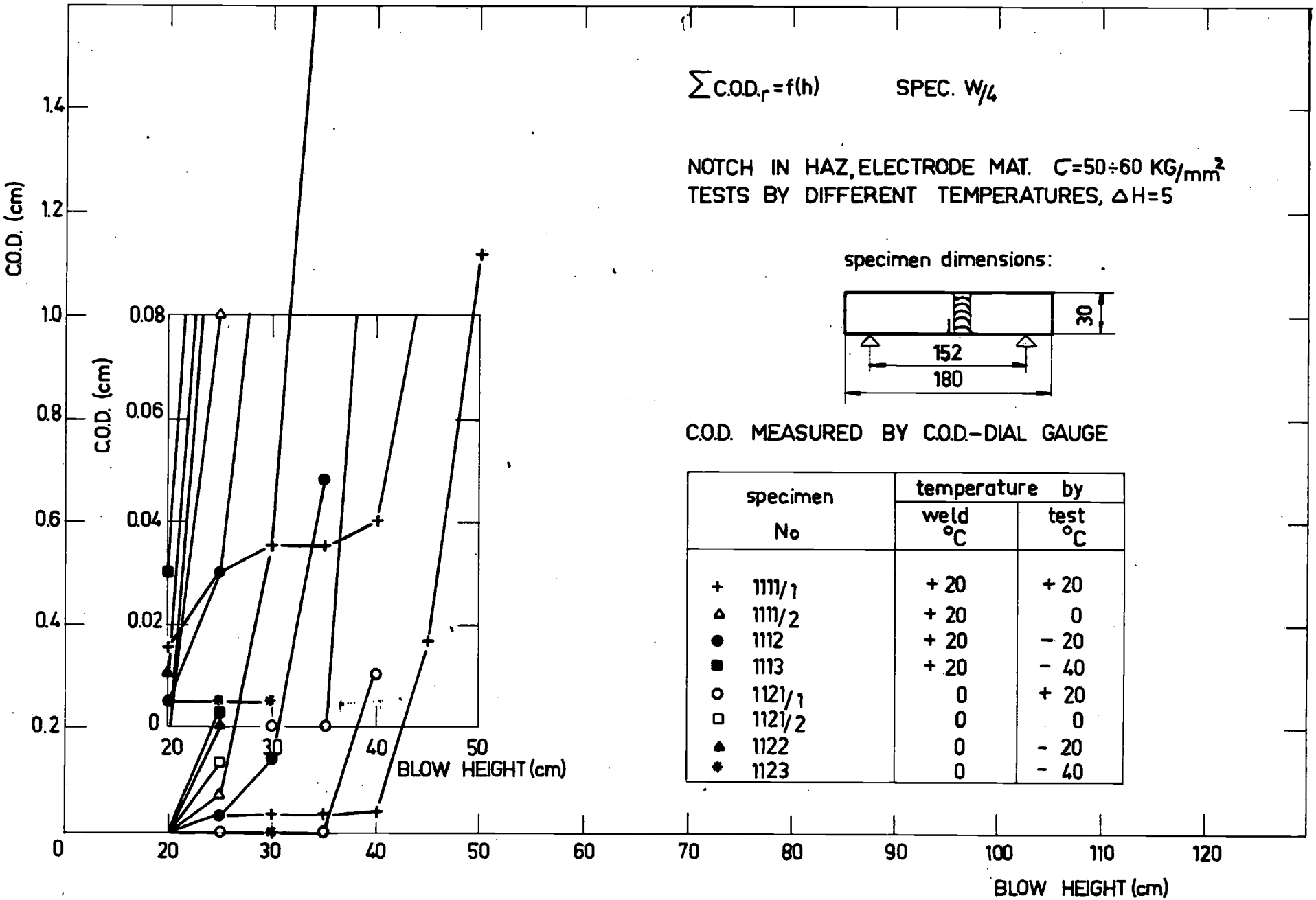

specimen No	temperature by weld °C	temperature by test °C
+ 1111/1	+ 20	+ 20
△ 1111/2	+ 20	0
● 1112	+ 20	− 20
■ 1113	+ 20	− 40
○ 1121/1	0	+ 20
□ 1121/2	0	0
▲ 1122	0	− 20
✱ 1123	0	− 40

FIG. 41. Residual value of the COD as function of the height of the blow. Results of the tests of the welded specimens group W/4.